INFORMATION TO USERS

This manuscript has been reproduced from the microfilm master. UMI films the text directly from the original or copy submitted. Thus, some thesis and dissertation copies are in typewriter face, while others may be from any type of computer printer.

The quality of this reproduction is dependent upon the quality of the copy submitted. Broken or indistinct print, colored or poor quality illustrations and photographs, print bleedthrough, substandard margins, and improper alignment can adversely affect reproduction.

In the unlikely event that the author did not send UMI a complete manuscript and there are missing pages, these will be noted. Also, if unauthorized copyright material had to be removed, a note will indicate the deletion.

Oversize materials (e.g., maps, drawings, charts) are reproduced by sectioning the original, beginning at the upper left-hand corner and continuing from left to right in equal sections with small overlaps. Each original is also photographed in one exposure and is included in reduced form at the back of the book.

Photographs included in the original manuscript have been reproduced xerographically in this copy. Higher quality 6" x 9" black and white photographic prints are available for any photographs or illustrations appearing in this copy for an additional charge. Contact UMI directly to order.

UMI

A Bell & Howell Information Company
300 North Zeeb Road, Ann Arbor MI 48106-1346 USA
313/761-4700 800/521-0600

FLOW AND DRYING CHARACTERISTICS OF A NOVEL ROTATING JET ANNULAR SPOUTED BED

Sakamon Devahastin

Department of Chemical Engineering
McGill University
Montreal, Quebec, Canada

A thesis submitted to the Faculty of Graduate Studies and Research in partial fulfillment of the requirements for the degree of Master of Engineering

National Library
of Canada

Acquisitions and
Bibliographic Services

395 Wellington Street
Ottawa ON K1A 0N4
Canada

Bibliothèque nationale
du Canada

Acquisitions et
services bibliographiques

395, rue Wellington
Ottawa ON K1A 0N4
Canada

Your file Votre reference

Our file Notre référence

0-612-29590-7

Canada

ABSTRACT

Due to several limitations encountered with the conventional spouted bed, a novel gas-solid contactor, Rotating Jet Annular Spouted Bed (RJASB), was developed for drying of particulates in the falling rate period. This contactor consists of one rotating jet in the annular region with a cylinder mounted centrally in the vessel. The key hydrodynamic characteristics, e.g., minimum spouting velocity, peak and steady spouting pressure drops were measured using different particles. Effects of the spouting jet rotational speed, bed height, nozzle diameter as well as particle size, shape and density were determined experimentally. Empirical correlations are developed to predict the values of these quantities.

Drying kinetics were studied using rewetted wheat as the test material. Effects of inlet air temperature and bed height on drying rates in the RJASB were studied. Both experimental and finite element simulation results were used to develop a new correlation for the effective water diffusion coefficient in wheat based on a two-dimensional diffusion model.

RÉSUMÉ

Vue les multiples limitations rencontrèes avec le lit jaillissant usuel, un nouveau contacteur gaz-solide, le lit jaillissant à jet rotatif annulaire (RJASB), a été développé pour le séchage particumaire durant la séquence de chute. Ce contacteur consiste en un jet rotatif à l'intérieur de la région annulaire avec un cylindre monté centralement à l'intérieur de l'appareil.

Les principales caractéristiques hydrodynamiques, c.à.d., vitesse minimale de jaillissement, pic et étude de chute de pression du jet furent mesurées en utilisant différentes particules. Des effets de vitesse rotative du jet, position haute, diamétre du nez ainsi que la taille des particules, forme et densité ont été déterminés expérimentalement. Des corrélations empiriques ont été développées afin de déterminer les valeurs de ces paramètres.

La cinétique de séchage a été étudiée en utilisant du blé humidifié comme matière d'expérimentation. Des effets de températures de l'air à l'entrèe et en position haute sur la séquence de séchage à l'intérteur du RJASB furent étudiées. L'ensemble des résultats de simulations expérimentales et des éléments finis ont été utilisés pour développer une nouvelle correlation pour le coefficient de diffusion effectif de l'eau dans le blé, basée sur un modèle de diffusion en deux dimensions.

ACKNOWLEDGMENTS

I would like to express my veracious thanks to my academic advisor, Professor A.S. Mujumdar, for his excellent and consistent suggestions, ideas and encouragement. My grateful is also given to Professor G.S.V. Raghavan of the Agricultural Engineering Department for his kind support during the course of this research.

I would like also to give my sincere appreciation to my friend Z.X. Gong for his invaluable suggestions on both theoretical and experimental viewpoints of this work. Thanks also to S. Sotocinal for his assistant in equipment installation and modification. Also thanks to the members of the Chemical Engineering Department particularly Mr. A. Gagnon for their help in the fabrication of the machine parts.

Acknowledgment is also due to my uncle Harold Hewett and my friend M. Gumputhram for their help in preparation of the French abstract.

Last, but certainly not least, I am vastly indebted to my parents for their love and endless sacrifices. Thanks also to my aunt and her family for their kind support during my stay in Montreal. Finally, I would like to give my sincere thanks to my best friend, P. Suwanruji, for her consistent encouragement while being away from home.

TABLE OF CONTENTS

Chapter 3 Experimental Set-up, Materials and Methodology

Chapter 4 Hydrodynamic Characteristics of the Rotating Jet Annular Spouted Bed

LIST OF FIGURES

Chapter 3 Experimental Set-up, Materials and Methodology

Chapter 4 Hydrodynamic Characteristics of the Rotating Jet Annular Spouted Bed

Chapter 5 Drying Kinetics in the Rotating Jet Annular Spouted Bed : Experimental Results and Mathematical Model

Appendix I : A Colorimetric Technique to Quantify Wheat Grain Damage During Drying

LIST OF TABLES

Chapter 2 Background

Chapter 3 Experimental Set-up, Materials and Methodology

Chapter 4 Hydrodynamic Characteristics of the Rotating Jet Annular Spouted Bed

Chapter 5 Drying Kinetics in the Rotating Jet Annular Spouted Bed : Experimental Results and Mathematical Model

Chapter 1

Introduction

1.1 General Introduction

The terms ***spouted bed*** and ***spouting*** were coined at the National Research Council of Canada in 1954 by Mathur and Gishler [1]. These investigators developed this technique initially as a method for drying wheat. Realizing that the technique could have wider application studies of the characteristics of a spouted bed using a variety of particulate materials with both air and water as the spouting medium have been implemented. On the basis of this preliminary study it was able to assert that the mechanism of flow of solids as well as gas in this technique is different from fluidization, but it appears to achieve the same purpose for coarse particles as fluidization does for fine particles.

Due to several limitations of the conventional spouted bed (CSB) [2], which is one of the reasons for the limited commercial use of spouted bed compared to fluidized bed, many modified spouted beds have been developed [3,4] to overcome some of the limitations of CSBs. Among the most important limitations of the CSB one may cite high pressure drop prior to onset of spouting, low annulus aeration, slow solids turnover, low capacity per unit floor space and difficulty of scale-up.

For grains most of the resistance to drying is in the falling rate period [5,6,7]. Thus, the rates of internal heat and mass transfer within the kernel determine the overall drying rate. This implies that external convective heat/mass transfer need not be supplied at high intensity continuously with little penalty in terms of increased drying time. Thus, spouting may take place only "intermittently". This periodic spouting could include heat

input varying at a low frequency. This results in saving in air consumption as well as thermal energy [6]. Further, a larger dryer is possible since one or two nozzles can periodically spout the entire contents of a large vessel by rotating the nozzles at a low rotational speed.

On the basis of the aforementioned argument, Mujumdar [8] proposed a round vessel fitted with a slowly rotating distributor plate equipped with spouting holes to supply heated gas to the bed either continuously or intermittently. The gas itself can be heated periodically, if necessary. The Rotating Jet Spouted Bed (RJSB) tested by Jumah [9] on a laboratory scale proved that Mujumdar's basic concept is valid. This spouted bed is a flat-base cylindrical column with a rotating inlet air distributor with two radially located nozzles which provide an on/off operation over the entire area of the bed.

Though several advantages are noted for RJSB, there are still some shortcomings [3]. Among the limitations are its complex construction, higher expected maintenance costs and limitations due to the maximum spoutable bed height. The objective of the present research is to develop a new spouted bed design to overcome some of these limitations. The Rotating Jet Annular Spouted bed (RJASB) consists of one rotating jet in the annular region. Any dead area in the central region of the bed is eliminated in this design. The slight reduction in bed capacity as compared to RJSB at the same bed height (approximately 17.5 percent) is offset by its simpler fabrication and modeling. It also requires less air flowrate for onset of spouting at a fixed value of distributor rotational speed. Thus allowing use of a deeper bed of the material to be processed.

1.2 Objectives

The motivation of this research was to develop and investigate a novel gas-solid contacting system viz. the rotating jet annular spouted bed. The major objectives of this work were :

1. To develop a novel gas-solid contactor based on the intermittent spouting concept.
2. To investigate the hydrodynamics of the system using different particulate materials.
3. To study the drying kinetics of rewetted wheat and estimate the effective moisture diffusion coefficient based on a two-dimensional liquid diffusion model using finite element method.

1.3 Thesis Layout

This thesis is divided into six chapters of which this introduction is the first. In Chapter 2, an introduction to the spouted bed design variations and modifications as well as a brief review of the relevant drying models are presented. Chapter 3 describes the experimental set-up, materials and methodology employed in this study. The hydrodynamic behavior of the RJASB is illustrated in Chapter 4. Chapter 5 discussed the drying characteristics of RJASB. Both the experimental results and mathematical model are presented. Finally, Chapter 6 presents conclusions of this research.

References

1. Mathur, K.B., Epstein, N., 1974, "*Spouted Bed*", Academic Press, New York.
2. Passos, M.L., Mujumdar, A.S., Raghavan, V.G.S., 1987, "Spouted Bed for Drying : Principles and Design Considerations", pp.359-398, in A.S. Mujumdar (ed.) *Advances in Drying, Vol. 4*, Hemisphere Publishing Corp., New York.
3. Devahastin, S., Mujumdar, A.S., Raghavan, G.S.V., 1996, "Spouted Beds Research at McGill University", *Proceedings of the International Conference on Food Industry Technology and Energy Applications*, Bangkok, Thailand, pp. 22-29.
4. Mujumdar, A.S., 1984, "Spouted Bed Technology - A Brief Review", in A.S. Mujumdar (ed.) *Drying' 84*, Hemisphere-McGraw-Hill, New York, pp. 151-157.

5. Becker, H.A., Sallans, H.R., 1960, "Drying Wheat in a Spouted Bed : On the Continuous Moisture Diffusion Controlled Drying of Solid Particles in a Well-mixed, Isothermal Bed", *Chem. Eng. Sci.*, 13, pp. 97-112.
6. Jumah, R.Y., Mujumdar, A.S., Raghavan, G.S.V., 1996, "A Mathematical Model for Constant and Intermittent Batch Drying of Grains in a Novel Rotating Jet Spouted Bed", pp.339-380, in I. Turner, A.S. Mujumdar (eds.) *Mathematical Modelling and Numerical Techniques in Drying Technology*, Marcel Dekker, New York.
7. Gong, Z.X., Devahastin, S., Mujumdar, A.S., 1997, "A Two-Dimensional Finite Element Model for Wheat Drying in a Novel Rotating Jet Spouted Bed", *Drying Technology-An International Journal*, 15(2), pp.575-592.
8. Mujumdar, A.S., 1989, "Recent Developments in Spouted Bed Drying", *Keynote Lecture, Transport Processes in Porous Media Conference*, Sao Carlos, S.P., Brazil.
9. Jumah, R.Y., 1995, "Flow and Drying Characteristics of a Rotating Jet Spouted Bed", Ph.D. Thesis, McGill University, Canada.

Chapter 2

Background

2.1 Introduction

This chapter presents a brief review of the literature relevant to the research subject. The progress in spouted bed technology, e.g., novel designs, research concepts and results are surveyed and reported. Mathematical models for drying of particulates, their theoretical basis, limitations and modifications are also reviewed and summarized.

2.2 Modified Spouted Bed

In order to put the work in perspective a generalized classification of spouted beds which shows schematics and key features of the devices is presented in Table 2.1. These modifications are concerned with changes in the vessel geometry, spouting operation and mechanism, air supply etc. Not all designs have potential industrial significance however.

Table 2.1 Classification of Spouted Beds [1]

CLASSIFICATION CRITERION	CONFIGURATION
I. Mechanism of spouting	• Pneumatic (e.g., CSB, draft tube SB) • Mechanical (e.g., screw conveyor SB) • Vibratory (e.g., vibro-spouted bed)
II. Vessel geometry	• Cylindrical-conical (CSB) • Conical • Flat Bottom • Rectangular

III. Flow configurations of particles in the bed	• Axisymmetric (CSB, conical) • Two-dimensional • Three dimensional
IV. Air entry	• Single nozzle at bottom • Central nozzle with auxiliary flow along the annulus • Tangential or swirling air entry along periphery • No air (vibro-spouted bed) • Multiple nozzles • Rotating nozzles • Rotating-impinging nozzles
V. Spouting air flow	• Continuous • Pulsed or intermittent
VI. Internals	• With draft tube or divider plates • Active internals (screw conveyor) • No internals (CSB)
VII. Operational mode	• Batch • Continuous • Multi-stage
VIII. Bed particles	• Active • Inactive (e.g., drying of pastes or slurries)
IX. Combined modes	• Spout-fluid bed • Fluid-spout bed • Jet spouted bed • Rotating jet spouted bed • Rotating-impinging jet spouted bed
X. Spouting fluid phase	• Two-phase spouting (gas-solid, liquid-solid, liquid-liquid)

	• Three-phase spouting (gas-solid-liquid)
XI. Heat input	• Convective • Combined conduction/convection

Studies of modified spouted bed included both extensive experimentation and phenomenological modelling. Numerous studies on hydrodynamics, heat/mass transfer as well as system applications were reported in the literature. Lim and Grace [2] studied flow characteristics in a flat-based half cylindrical column of diameter 0.91 m with different inlet orifice and particle sizes. These investigators found that the correlations for minimum spouting velocity developed on small vessels generally gave poor predictions for the large diameter vessel. They also showed that in order to achieve stable spouting it is necessary to operate with inlet orifice diameter less than 30 times the mean particle diameter.

He et.al. [3] used fibre optic probe to measure voidage profiles in the fountain, spout and annulus of spouted beds. They indicated that the voidage in most of the annulus was somewhat higher than the loose-packed voidage and increased with increasing spouting gas flowrate, contrary to usual assumptions. They also found that the radial profiles of local voidage were roughly parabolic in the lower portion of the spout and blunt in the upper region. He et.al. [4] later employed the same technique to measure the profiles of vertical particle velocities in the spout and fountain of a half-column and full-column spouted beds. They found that the flat plate in half-column geometry strongly affects particle velocities. Hence data obtained by observing particle motion at the outer wall tend to be misleading as indicators of particles velocities elsewhere in the annulus. Roy et.al. [5] also reported the distortion of hydrodynamic behavior by a curtain effect in semi-cylindrical columns which is absent in full columns. They also pointed out some disadvantages of using fibre optic measurements in spouted bed, such as flow disturbance due to insertion of probes in the reactor. These investigators then developed a non-invasive γ-ray emission system to follow the motion of a single radioactive particle in a

three-dimensional spouted bed reactor. They were able to use this technique to determine the average particle velocity field and other hydrodynamic quantities which could not be evaluated accurately using any other technique.

Olazar et.al.[6] studied flow behavior of nearly flat base spouted beds and reported different characteristics from those of the conventional spouted beds with conical base. They also developed empirical correlations for calculation of the minimum spouting velocity, peak and steady spouting pressure drops. It is also reported that the effect of the base angle is more important in shallow beds than deeper beds.

Krzywanski et.al. [7] proposed a multi-dimensional model to describe the fluid and particle dynamic behaviour of spouted beds. They were able to predict some key hydrodynamic characteristics which were found to be in reasonable agreement with available experimental results selected from literature. Hattori et.al. [8] also developed similar model based on Ergun's equation which allowed them to derive the general expression for the longitudinal distributions of fluid velocity and pressure in the annulus.

Studies on heat/mass transfer in spouted beds also received considerable attention from various investigators. Rocha et.al. [9] studied aerodynamics and heat transfer in two-dimensional spouted bed as applied to coating process. Freitas and Freire [10] studied experimentally wall-to-bed and fluid-to-particle heat transfer coefficients in spouted bed. They also proposed a new definition of wall-to-bed heat transfer coefficient based on experimental observations. Kudra et.al. [11] studied experimentally the hydrodynamics, heat transfer and drying characteristics of two-dimensional spouted bed with and without draft channel. Empirical correlations for key hydrodynamic parameters as well as heat transfer coefficient and drying rate were then developed for the design and scale-up purposes. Jumah et.al. [12] studied different heating and spouting schemes in a novel rotating jet spouted bed and showed that significant energy and quality advantages may accrue from intermittent drying of heat sensitive particles. Summaries of research results and applications of spouted beds may be found in [13-15].

2.3 Drying Models

Drying, especially as applied to food and biological products, is a widely applied process for different purposes, e.g., increasing shelf-life, reducing packing costs, lowering shipping weights, improving sensory attributes as well as encapsulating flavors and preserving nutritional value. Several review articles have recently been presented on the topic of drying. Waananen et.al. [16] provide a comprehensive review of current drying theories with identification key characteristics of models including controlling process resistance, internal mechanisms of moisture movement, methods of model coefficient determination as well as model solution and validation. The volume of literature published annually on modeling of drying, however, indicates that the fundamental mechanisms of drying are not completely understood and that material-specific physicochemical transitions during drying play an important role in determining process mechanisms. The latter reason is frequently used as a justification for developing empirical and system specific models [17].

For materials undergoing falling rate period drying, in particular grains, diffusion based theories are fairly popular [17]. A compelling reason for the popularity is their simplicity. The material properties and the material-solvent interactions are lumped into a single effective diffusivity which is determined experimentally through drying experiments.

Becker and Sallans [18] reported a study of the basic variables involved in the drying of wheat kernels in a stream of dry, isothermal air. A correlations of the data was developed by assuming the applicability of the diffusion model in an equivalent sphere. While the method afforded a practical solution, Becker [19] pointed out that it is just a theoretically unsatisfying substitute for a general approach to the rigorous treatment of unsteady diffusion in solids of geometry too complex to allow analytical integration of the differential diffusion equation and leads to an indeterminate error in the calculation of the diffusion coefficient. This investigator then proposed a mathematical method for the general solution of problems of unsteady diffusion in solids of arbitrary shape and, in

particular, to wheat. It was reported that the drying rate predicted by the integral solution is only slightly lower than the experimental results when the wheat particle is modeled as a sphere.

Fortes et.al. [20] developed a coupled heat and mass transfer model for wheat drying based on irreversible thermodynamics. In fact, their model is a modified version of Luikov's model. Theoretically, their model describes more accurately the physics of the heat and mass transfer processes than does a simple liquid diffusion model. However, the applicability of their model is greatly limited due to the fact that the governing equations include many coefficients which are very difficult to determine experimentally.

Numerical simulations play an important role in the study of grain drying process. Bakker-Arkema was among the first to propose a computer simulation model for crop drying [21]. These mathematical equations which are in differential form and based on the conservation of heat and mass have been used widely for design and analysis of crop dryers. Parry [22] presented a review of the mathematical and simulation models used for grain drying. Irudayaraj et.al. [23] employed a finite element procedure to solve two sets of non-linear coupled equations which consider temperature and moisture dependent material properties. A recommendation for the selection of one model over the others cannot be made based on their results since accurate values for some of the material properties are not available.

For drying in spouted beds, Becker and Sallans [24] performed an experimental study of wheat drying in a spouted bed. They modeled the wheat particle as a sphere and obtained a correlation for the drying rate of wheat kernel based on the liquid diffusion theory. They also presented a correlation for the critical grain temperature above which the baking qualities of dried wheat are impaired. Zahed and Epstein [25] presented a complete set of equations with no adjustable parameters for numerically predicting the variation of grain temperature and moisture content with time for batch drying as well as exit grain and air moisture contents along with temperatures for continuous drying in

spouted bed. The model proved to give a good representation of drying process in spouted bed of cereal grains. They also pointed out the need for a reliable equations for predicting effective diffusivity which are scarce for cereal grains. Jumah et.al. [12] performed intermittent heating and spouting in a novel rotating jet spouted bed and showed that significant energy and quality advantages may accrue from intermittent drying of heat sensitive particles. Gong et.al. [26] pointed out the inappropriateness of modelling wheat as a spherical body. These investigators showed the deviation in drying results obtained by using the correlation for effective diffusion coefficient developed by assuming spherical geometry in their two-dimensional liquid diffusion model. Thus, a more realistic value of the effective diffusion coefficient is needed if the drying object is modelled more accurately in terms of its geometry.

For a detailed discussion of spouted bed drying the reader is referred to the chapter on spouted bed drying in the Handbook of Industrial Drying [27].

References

1. Devahastin, S., Mujumdar, A.S., Raghavan, G.S.V., 1996, "Spouted Beds Research at McGill University", *Proceedings of the International Conference on Food Industry Technology and Energy Applications*", Bangkok, Thailand, pp.22-29.
2. Lim, C.J., Grace, J.R., 1987, "Spouted Bed Hydrodynamics in a 0.91 m Diameter Vessel, *Can. J. Chem. Eng.* 65, pp. 366-372.
3. He, Y.L., Lim, C.J., Grace, J.R., Zhu, J.X., Qin, S.Z., 1994, "Measurements of Voidage Profiles in Spouted Beds", *Can. J. Chem. Eng.*, 72, pp. 229-234.
4. He, Y.L., Qin, S.Z., Lim, C.J., Grace, J.R., 1994, "Particle Velocity Profiles and Solid Flow Patterns in Spouted Beds", *Can. J. Chem. Eng.*, 72, pp. 561-568.
5. Roy, D., Larachi, F., Legros, R., Chaouki, J., 1994, "A Study of Solid Behavior in Spouted Beds Using 3-D Particle Tracking", *Can. J. Chem. Eng.*, 72, pp. 945-952.

6. Olazar, M., San Jose, M.J., Aguayo, A.T., Arandes, J.M., Bilbao, J., 1994, "Hydrodynamics of Nearly Flat Base Spouted Beds", *Chem. Eng. J.*, 55, pp. 27-37.
7. Krzywanski, R.S., Epstein, N., Bowen, B.D., 1992, "Multi-Dimensional Model of a Spouted Bed", *Can. J. Chem. Eng.*, 70, pp. 858-872.
8. Hattori, H., Matsuse, T., Fukuhara, K., 1992, "Force Balance Model of the Spouted Bed for Non-Darcy Flow in the Annulus", *J. Chem. Eng. Japan.*, 25, pp. 655-660.
9. Rocha S.C.S., Taranto, O.P., Ayub, G.E., 1995, "Aerodynamics and Heat Transfer During Coating of Tablets in Two-Dimensional Spouted Bed", *Can. J. Chem. Eng.*, 73, pp. 308-312.
10. Freitas, L.A.P., Freire, J.T., 1993, "Heat Transfer in Spouted Beds", *Drying Technology-An International Journal*, 11, pp. 303-317.
11. Kudra, T., Mujumdar, A.S., Raghavan, G.S.V., Kalwar, M.I., 1992, "Two-Dimensional Spouted Beds : Some Hydrodynamic, Heat Transfer and Drying Characteristics", pp. 65-85, in A.S. Mujumdar (ed.) *Drying of Solids*, International Science Publisher, New York.
12. Jumah, R.Y., Mujumdar, A.S., Raghavan, G.S.V., 1996, "A Mathematical Model for Constant and Intermittent Batch Drying of Grains in a Novel Rotating Jet Spouted Bed", *Drying Technology-An International Journal.*, 14, pp. 765-802.
13. Passos, M.L., Mujumdar, A.S., Raghavan, G.S.V., 1987, "Spouted Beds for Drying : Principles and Design Considerations", pp.259-397, in A.S. Mujumdar (ed.) *Advances in Drying, Vol.4*, Hemisphere Publishing, New York.
14. Mujumdar, A.S., 1984, "Spouted Bed Technology-A Brief Review", pp. 151-157, in A.S. Mujumdar (ed.) *Drying '84*, Hemisphere McGraw-Hill, New York.
15. Mathur, K.B., Epstein, N., 1974, "*Spouted Bed*", Academic Press, New York.
16. Waananen, K.M., Litchfield, J.B., Okos., M.R., 1993, "Classification of Drying Models for Porous Solids", *Drying Technology-An International Journal.*, 11, pp. 1-40.
17. Achanta, S., Okos, M.R., 1996, "Predicting the Quality of Dehydrated Foods and Biopolymers - Research Needs and Opportunities", *Drying Technology-An International Journal.*, 14, pp. 1329-1368.

18. Becker, H.A., Sallans, H.R., 1955, "A Study of Internal Moisture Movement in the Drying of the Wheat Kernel", *Cereal Chem.*, 32, pp. 212-226.
19. Becker, H.A., 1959, "A Study of Diffusion in Solids of Arbitrary Shapes, with Application to the Drying of the Wheat Kernel", *J. Appl. Poly. Sci.*, 1, pp.212-226.
20. Fortes, M., Okos, M.R., Barrett, Jr., J.R., "Heat and Mass Transfer Analysis of Intra-Kernel Wheat Drying and Rewetting", *J. Argic. Engng. Res.*, 26, pp. 109-125.
21. Sokhansanj, S., Raghavan, G.S.V., 1996, "Drying of Grains and Forages : A Brief Review of Recent Advances", *Drying Technology-An International Journal.*, 14, pp. 1369-1380.
22. Parry, J.L., 1985, "Mathematical Modelling and Computer Simulation of Heat and Mass Transfer in Agricultural Grain Drying : A Review", *J. Argic. Engng. Res.*, 32, pp. 1-29.
23. Irudayaraj, J., Haghighi, K., Stroshine., R.L., 1992, "Finite Element Analysis of Drying with Application to Cereal Grains", *J. Argic. Engng. Res.*, 53, pp. 209-229.
24. Becker H.A., Sallans, H.R., 1960, "Drying Wheat in a Spouted Bed : On the Continuous Moisture Diffusion Controlled Drying of Solid Particles in a Well-Mixed, Isothermal Bed", *Chem. Eng. Sci.*, 13, pp.97-112.
25. Zahed, A.H., Epstein, N., 1992, "Batch and Continuous Spouted Bed Drying of Cereal Grains : The Thermal Equilibrium Model", *Can. J. Chem. Eng.*, 70, pp.945-953.
26. Gong, Z.X., Devahastin, S., Mujumdar, A.S., 1997, "A Two-Dimensional Finite Element Model for Wheat Drying in a Novel Rotating Jet Spouted Bed", *Drying Technology-An International Journal*, 15(2), pp. 575-592.
27. Pallai, E., Szentmarjay, T., Mujumdar, A.S., 1995, "Spouted Bed Drying", pp.453-488, in A.S. Mujumdar (ed.) *Handbook of Industrial Drying, 2nd ed.*, Marcel Dekker, Inc., New York and Basel.

Chapter 3

Experimental Set-up, Materials and Methodology

3.1 Introduction

This chapter provides details about the experimental set-up, the design of the rotating jet annular spouted bed (RJASB), the materials used, the experimental procedure as well as the techniques employed in the hydrodynamic and drying experiments. Experimental reproducibility results are also presented.

3.2 Experimental Set-up

A schematic diagram of the experimental set-up and the associated instrumentation is given in Figure 3.1. The RJASB is realized by using a slowly rotating inlet air distributor plate equipped with a nozzle under the bed supporting screen. The nozzle (2.0 and 3.0 cm in diameter) is located at 18 cm from the center of the vessel. The distributor is enclosed within a sealed aluminum box. The supporting screen is made of galvanized steel wire (2×2 mesh) reinforced along its circumference by a circular metal loop. This main support screen is covered at the upper surface with a 20×20 mesh aluminum wire net. The openings of the finer screen are small enough to contain the particles but large enough so that flow of air is essentially unrestricted.

The rotating section of the main inlet air pipe is provided on its outer surface with two rubber sealed ball bearing assemblies ; all are circumfused by another well sealed coaxial pipe. The downstream part of this rotating section is engaged with two belt-driven pulleys connected to a 3-hp variable speed AC motor (Boston Gear, Quincy, MA) through a gear speed reducer (Boston Gear, Quincy, MA) calibrated with a digital tachometer.

The spouted bed consists of a cast acrylic vessel 45 cm in diameter and 60 cm in height. A galvanized steel cylinder, 20 cm diameter and 55 cm height, with the top 5 cm perforated, is mounted centrally in the vessel. In order to prevent entrainment of particles from the bed, a wooden cover plate is installed at the top of the vessel with 4 opening holes of equal size (7.5 cm diameter) to minimize pressure build up in the vessel.

The spouting air was supplied by a high pressure blower (GAST Regenair, model no. R7100 B-1, GAST Mfg. Corp., Benton Harbor, MI) and maintained at the pre-selected temperatures by a set of electric heaters rated at 4.5 kW fitted with P controller. The outer wall of the heating compartment is insulated with fiberglass to minimize heat losses. The air flowrate was measured with a precalibrated pitot tube (model no. FPT 6120, Omega Engineering, Inc., Stamford, CT) and regulated by mean of gate valve on the feed line. Differential pressure drop across the pitot tube was measured using a manometer filled with a manometric fluid (Meriam 100 fluid, Meriam Instrument, Cleveland, OH).

Pressure drop across the bed was measured using static pressure taps connected to a manometer filled with a manometric fluid (Meriam 295 fluid, Meriam instrument, Cleveland, OH). The pressure taps are stainless steel with an internal diameter of 3 mm and an external diameter of 6 mm. The upstream pressure tap is placed below the gas inlet aperture in the entrance pipe. This procedure produces a positive pressure drop when running the column without the solids at the spouting gas rates [1]. The downstream tap is placed at the center of the upper end of the inner cylinder in order to prevent any fluctuation due to the rotating action of an inlet air nozzle.

Inlet air temperature as well as bed temperatures at different locations were measured using copper-constantan type T thermocouples (Omega Engineering, Inc., Stamford, CT). Thermocouples signals were acquired by a scanning thermocouple thermometer (model no. 92800-10, Cole-Parmer Instrument Co., Barrington, IL).

Rotating Jet Annular Spouted Bed

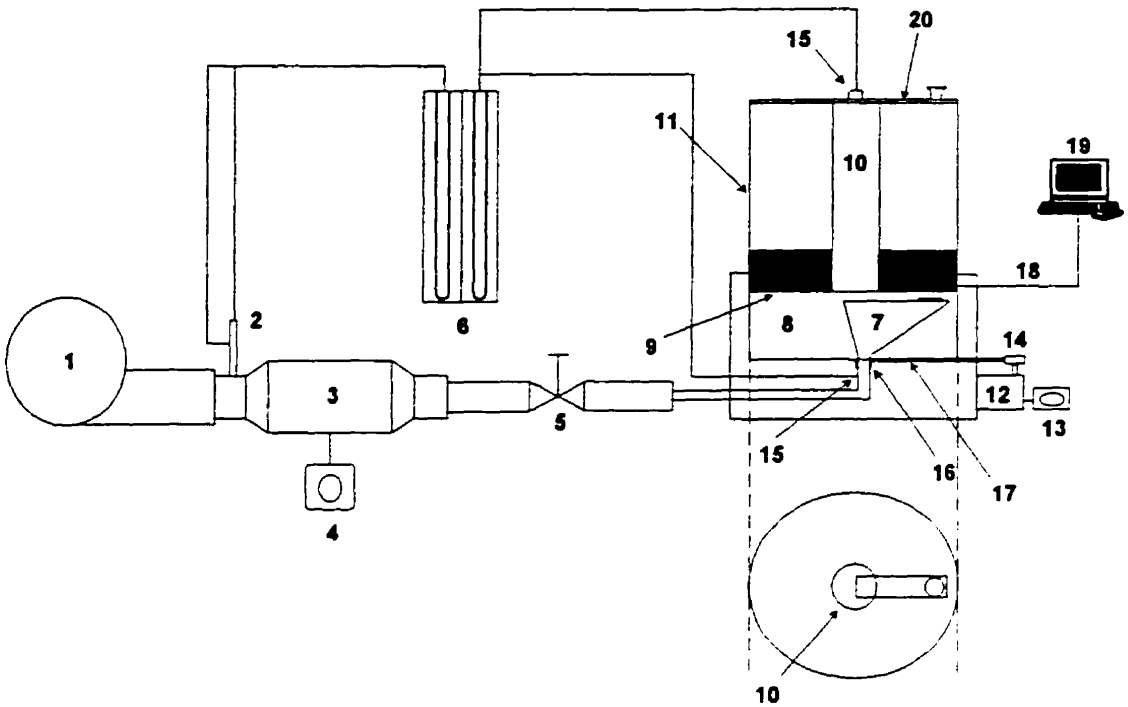

Item no.	Description	Item no.	Description
1	Air blower	11	Vessel
2	Pitot tube	12	Motor + gear box
3	Electric heater	13	Motor controller
4	P controller	14	Pulley
5	Gate valve	15	Pressure taps
6	Manometers	16	Ball bearings
7	Air distributor	17	V-belt
8	Distributor cover	18	Thermocouples
9	Screen	19	STT[1]
10	Central cylinder	20	Cover plate

1. Scanning thermocouple thermometer

Figure 3.1. Schematic diagram of the overall experimental apparatus

3.3 Materials

Soft Spring wheat, corn and polystyrene pellets were used as the test materials in the aerodynamic experiments while for the drying kinetics experiments, rewetted wheat was used. Following Geldart's classification [2], all particles used in this work belong to group D (spoutable, large and dense particles). Dimensions and physical properties (average values) of the particles tested are given below in Tables 3.1-3.3.

The particle dimensions, length (L), breadth (B), and thickness (Z), were measured using a digital calliper (Digimatic Calliper, Mitutoyo Corporation, Japan) having a least count of 0.01 mm. Two hundred particles were measured for each type of material. The bulk density, ρ_b, was determined by pouring a weighed amount of sample particles through a funnel into a measuring cylinder. The volume occupied by the sample was then used to determine the values of the loose bulk density. The particle density, ρ_s, was estimated using fluid displacement with water as measuring fluid. An electronic balance accurate to ± 0.001 g was used in weight determination.

Table 3.1 Dimensions of Particles Used in the Aerodynamic Experiments

Material	L (mm)	B (mm)	Z (mm)	D_{p_e} [1] (mm)	$D_{p_{gm}}$ [2] (mm)	D_p [3] (mm)	ϕ [4] (-)
Polystyrene	3.331	3.004	2.296	3.527	2.842	3.009	0.853
Wheat							
(rewetted)	5.863	3.056	2.639	4.486	3.616	2.763	0.616
(dried)	5.295	3.158	2.732	4.435	3.575	2.994	0.675
Corn	10.567	7.985	4.770	9.160	7.383	6.400	0.698

1 : Equivalent spherical diameter
2 : Geometric particle diameter = $(L \times B \times Z)^{1/3}$ [3]
3 : Effective particle diameter = $D_{p_e} \times \phi$
4 : Sphericity = $D_{p_{gm}} / L$ [3]

Table 3.2 Physical Properties of Bed Particles Used in Aerodynamic Experiments

Material	ρ_s (kg/m^3)	ρ_b (kg/m^3)	Ar (-)	U_t[1] (m/s)	ε[2] (-)
Polystyrene	1026.1	584.7	7.33×10^5	6.24	0.430
Wheat					
(rewetted)	1233.6	719.1	6.90×10^5	5.44	0.417
(dried)	1182.0	779.3	8.41×10^5	5.66	0.341
Corn	1227.5	764.6	8.52×10^6	8.53	0.377

1 : Calculated values [4]

2 : $\varepsilon = 1 - (\rho_b / \rho_s)$ [3]

Table 3.3 Physical Properties of Rewetted Wheat Used in Drying Experiments

Property	Value	Property	Value
L (mm)	5.863	ρ_s (kg/m^3)	1233.6
B (mm)	3.056	ρ_b (kg/m^3)	719.1
Z (mm)	2.639	Ar (-)	6.90×10^5
$D_{p_{sph}}$ (mm)	3.616	U_t (m/s)	5.44
D_p (mm)	2.763	ε (-)	0.417
D_{p_c} (mm)	4.486		
ϕ (-)	0.616		

3.4 Experimental Procedure

3.4.1 Aerodynamic Experiments

The bed was prepared in a standardized manner before starting each experiment in order to minimize any variation in the packing state which may arise during the filling of the vessel with particles. This was done by loading an estimated quantity of material into the bed, spouting for 5 minutes at a fixed value of distributor rotational speed (generally at 5 rpm), then increasing the rotational speed until the new flow regime is established, shut off the airflow and let the particles settle down and be re-packed.

The spouting regime, i.e., a plot of bed pressure drop versus superficial air velocity, was established by gradually increasing the air flowrate until a spout was formed. After steady spouting the air flowrate was gradually reduced until the spouting ceased. The air flowrate at which the fountain just collapsed was taken as the minimum spouting flowrate (Q_{ms}) for the given system combinations. The flow was then further reduced in steps to zero. The flowrate and total pressure drop were recorded simultaneously. The bed pressure drop was calculated using the expression given by Mathur and Epstein [1] with a slight modification. This is given below as equation (3.1).

$$\Delta P_{bed} = \sqrt{(\Delta P_{tot}^2 - \Delta P_{emp}^2)} \qquad (3.1)$$

The superficial and nozzle minimum spouting velocities were calculated from the total air flowrate, Q_{ms}, using the following expression :

$$U_{msc}(\text{or } U_{msn}) = \frac{4Q_{ms}}{\pi D^2} \qquad (3.2)$$

where D is the column diameter or nozzle diameter depending on the quantity investigated.

The range of experimental conditions employed were :

1. Distributor rotational speed (N) : 0-10 rpm.
2. Bed height (H) : 10-20 cm.
3. Nozzle diameter (D_n) : 2 and 3 cm.
4. Particles : polystyrene, wheat and corn.
5. Superficial air velocity (U_c) : 0-0.64 m/s

The dependent variables were :

1. Spouting regime (ΔP_{bed} vs. U).
2. Minimum spouting velocity (U_{ms}).
3. Peak pressure drop (ΔP_M).
4. Steady spouting pressure drop (ΔP_s).

3.4.2 Drying Kinetics Experiments

The drying kinetics were measured in the batch mode using rewetted wheat as the test material. After sieving out foreign materials, the wheat was rewetted by adding a pre-determined amount of tap water to achieve the required initial moisture content. The contents were mixed thoroughly while adding the water by the use of a small "concrete mixer". The grain was then placed in a sealed plastic container and kept in a cold storage room at 4 °C with periodic mixing for a minimum of 72 hours to ensure reproducible moisture adsorption and uniform distribution within the grain kernels.

Before the start of each experiment, the rewetted wheat was removed from cold storage and kept at ambient temperature for 24 hours to achieve thermal equilibration at ambient conditions. The experimental procedure was as follows :

1. The scanning thermocouple thermometer, blower, heaters and the motor (at fixed value of rotational speed) were switched on.
2. Hot air at pre-selected flowrate and temperature was passed through the empty vessel for thermal stabilization for about 1 hour.
3. When the steady state was reached, the air flow was diverted to the by-pass line and the selected weight of wet solids was loaded into the vessel.
4. Samples weighing 10 grams each were periodically taken out from the bed for moisture content determination following the ASAE standard [5].
5. The time-changes of the bed temperatures at different locations were recorded.

As indicated by various investigators [6,7] that wheat drying with an initial moisture content of less than 0.5 kg/kg (d.b.) is in the falling rate period, the main contributor to the variation of the drying curves turns out to be the inlet air temperature. Thus, in this experimental work, emphasis was placed on investigation of the effect of an inlet air temperature as well as the static bed height. The operating ranges of these two parameters along with the fixed values of others were as follows :

1. Inlet air tempearture (T_i) : 63-80 °C. The upper limit was suggested by the safe maximum allowable temperature for wheat drying [8] while the lower limit was determined by the flow system behavior.
2. Bed height (H) : 10-20 cm.
3. Distributor rotational speed (N) : fixed at 5 rpm.
4. Air superficial velocity (U_c) : fixed at 0.64 m/s.
5. Nozzle diameter (D_n) : fixed at 3 cm.

The dependent variables were :

1. Sample moisture content (X).
2. Bed Temperature (T_b) taken as an average values from measurements at different locations.

3.5 Note on Reproducibility of the Results

To investigate the reproducibility of the results, replicates were made of randomly selected experiments, both in the hydrodynamic and drying experiments. From these tests, the reproducibility values of U_{ms}, ΔP_S, ΔP_M and the drying curves were within ± 6.0, 8.2, 12.8 and 2.0 percent, respectively. The relatively high nonreproducibility in ΔP_M is related to the fact that the peak pressure drop is bed history-dependent [1]. Nevertheless, the results confirmed good reproducibility of the overall experimental technique.

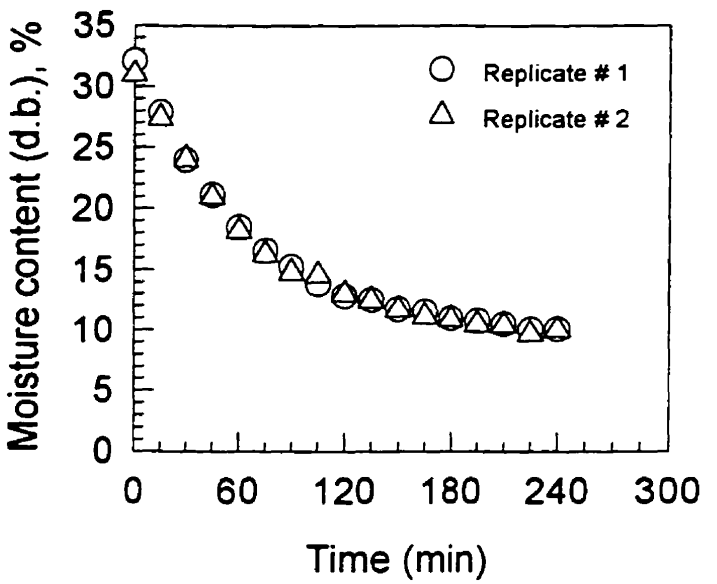

Figure 3.2. Reproducibility of the drying curves (rewetted wheat).
$T_i = 63$ °C, $D_n = 3$ cm, $H = 15$ cm, $N = 5$ rpm, $U = 0.64$ m/s, $X_0 \cong 0.30$kg/kg

Nomenclature

B	breadth, mm
D	diameter, mm

D_n	nozzle diameter, cm
D_p	effective particle diameter, mm
D_{p_e}	equivalent spherical diameter, mm
$D_{p_{gm}}$	geometric particle diameter, mm
g	gravitational constant, m s^{-2}
H	static bed height, cm
L	length, mm
N	rotational speed, rpm
ΔP_{bed}	bed pressure drop, kPa
ΔP_{emp}	empty vessel pressure drop, kPa
ΔP_M	peak pressure drop, kPa
ΔP_S	steady spouting pressure drop, kPa
ΔP_{tot}	total pressure drop, kPa
Q_{ms}	minimum spouting flowrate, m^3 s^{-1}
T_b	bed temperature, °C
T_i	inlet air temperature, °C
U	superficial velocity, m s^{-1}
U_{ms}	minimum spouting velocity, m s^{-1}
U_t	particle terminal velocity, m s^{-1}
X	moisture content, kg water per kg dry solid
Z	thickness, mm

Greek symbols

ε	voidage, $1-(\rho_b / \rho_s)$, no unit
ϕ	sphericity, $D_{p_{gm}} / L$, no unit
μ	viscosity, kg m^{-1} s^{-1}
ρ_b	bulk density, kg m^{-3}

ρ_s particle density, kg m^{-3}

Superscripts and subscripts

b	bulk, bed
c	column
g	gas
i	inlet
n	nozzle
p	particle
s	solid

Dimensionless groups

Ar Archimedes number, $\frac{D_p^3 \rho_g (\rho_s - \rho_g) g}{\mu_g^2}$

References

1. Mathur, K.B., Epstein, N., 1974, "*Spouted Bed*", Academic Press, New York.
2. Geldart, D., 1972, "Type of Gas Fluidization", *Powder Tech.*, 7, pp. 285-292.
3. Cenkowski, S., Zhang, Q., 1995, "Engineering Properties of Grains and Oilseeds", pp.411-463, in D.S. Jayas, N.D.G. White and W.E. Muir (eds.) *Stored-Grain Ecosystems*, Marcel Dekker, Inc., New York.
4. Sakiadis, B.C., 1984, "Fluid and Particle Mechanics", Section 5, in R.H. Perry, D.W. Green (eds.) *Perry's Chemical Engineers' Handbook, 6th ed.*, McGraw-Hill Book Co., New York.
5. ASAE Standards, 1989, *American Society of Agricultural Engineers*, St. Joseph, MI.
6. Becker, H.A., Sallans, H.R., 1960, "Drying Wheat in a Spouted Bed : On the Continuous Moisture Diffusion Controlled Drying of Solid Particles in a Well-mixed, Isothermal Bed", *Chem. Eng. Sci.*, 13, pp. 97-112.

7. Gong, Z.X., Devahastin, S., Mujumdar, A.S., 1997, "A Two-Dimensional Finite Element Model for Wheat Drying in a Novel Rotating Jet Spouted Bed", *Drying Technology-An International Journal*, 15(2), pp. 575-592.
8. Hall, C.W., 1980, "*Drying and Storage of Agricultural Crops*", AVI Publishing Company, Inc., Westport, Connecticut.

Chapter 4

Hydrodynamic Characteristics of the Rotating Jet Annular Spouted Bed

4.1 Introduction

Detailed knowledge of the hydrodynamic behavior in a spouted bed is important in ascertaining the effectiveness of gas-solid contact. Numerous works, both experimentation and phenomenological modelling, were devoted to the investigation of hydrodynamic characteristics in spouted beds. Most of the works, however, were carried out within the simple single-spout configurations column of 0.3 m or less [1].

Due to the fact that conventional spouted bed (CSB) suffers from several shortcomings [2] many modified spouted bed designs have been proposed and studied. Olazar et.al [3] studied the hydrodynamics of nearly flat base spouted beds and developed empirical correlations to predict some key hydrodynamic parameters important to the design and scale-up of their apparatus. Based on the fact that in the falling rate period drying the rates of internal heat/mass transfer determine the overall drying rate, Mujumdar [4] proposed the idea of supplying spouting air only intermittently for materials dry in this period. The Rotating Jet Spouted Bed (RJSB) tested by Jumah [5] on a laboratory scale proved that Mujumdar's basic concept is valid. This spouted bed is a flat-base cylindrical column with a rotating inlet air distributor consisting of two radially located nozzles which provide an on/off operation over the entire area of the bed. This investigator also showed that it is possible to double the column diameter used in his study (45 cm) without any instability problems.

Though several advantages are noted for the RJSB, there are still some shortcomings [6]. Among the limitations are its complex construction, higher expected maintenance costs and limitations due to the maximum spoutable bed height. The objective of the present research is to develop a new spouted bed design to overcome some of these limitations. The Rotating Jet Annular Spouted bed (RJASB) consists of one rotating jet in the annular region. Any dead area in the central region of the bed is eliminated in this design. The slight reduction in bed capacity as compared to RJSB at the same bed height (approximately 17.5 percent) is offset by its simpler fabrication and modeling. It also requires less air flowrate for onset of spouting at a fixed value of distributor rotational speed, thus allowing the use of a deeper bed of the material to be processed. The flow characteristics using different solid particulates was studied. Empirical correlations were developed to predict the key hydrodynamic characteristics of the system.

4.2 Spouting Mechanism

The mechanism of transition from a static to a spouted bed is best described with reference to a plot of bed pressure drop versus air velocity. Figures 4.1a,b,c show typical plots for rewetted wheat particles at an air distributor rotational speed of 0, 5 and 10 rpm, respectively. The plots are supplemented by branches illustrating the reverse process, that is the collapse of spout on decreasing the gas flowrate. Both superficial and jet velocities are specified since the latter seems to be of actual importance in spouting phenomenon.

The following sequence of events are observed as the flowrate is increased :

I. Increasing flow

Curve A$\rightarrow$B : As in conventional spouted bed, the pressure drop increases almost linearly with an increasing gas flowrate while the fixed-bed state remains unchanged. For stationary air distributor (Figure 4.1a), a small cavity is formed under the bed surface. In

the case of rotating air distributor (Figures 4.1 b and c), an internally relocated annular cavity is formed along the path of the rotating jet. An arch of compacted particles that offers high resistance to flow exists above the internal spout [7] so that the pressure drop across the bed rises further until reaches a maximum value at point B.

Curve B→C : As the flowrate is increased beyond point B, the height of the relatively hollow internal spout increases and the jet momentum is large enough to pierce the bed surface, hence spouting is onset. Pressure drops suddenly to point C.

Curve beyond C : With still further increase in gas flowrate, the additional gas simply passes through the spout region causing the fountain to shoot up higher without any significant effect on the pressure drop. The pressure drop beyond point C, therefore, remains substantially constant.

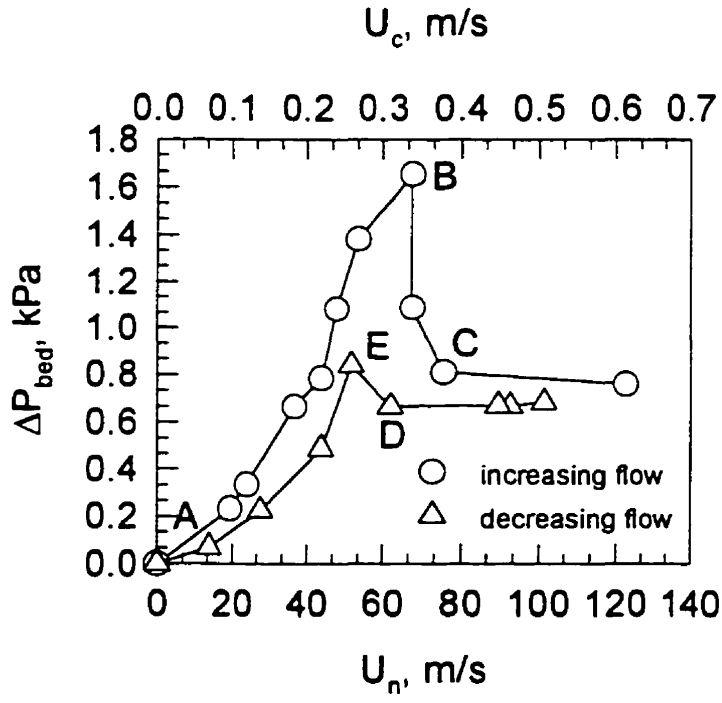

Figure 4.1a. Spouting characteristics for rewetted wheat particles, H = 15 cm, D_n = 3 cm, N = 0 rpm. B : peak pressure drop; C : onset of spouting; D : minimum spouting condition; E : spout collapse.

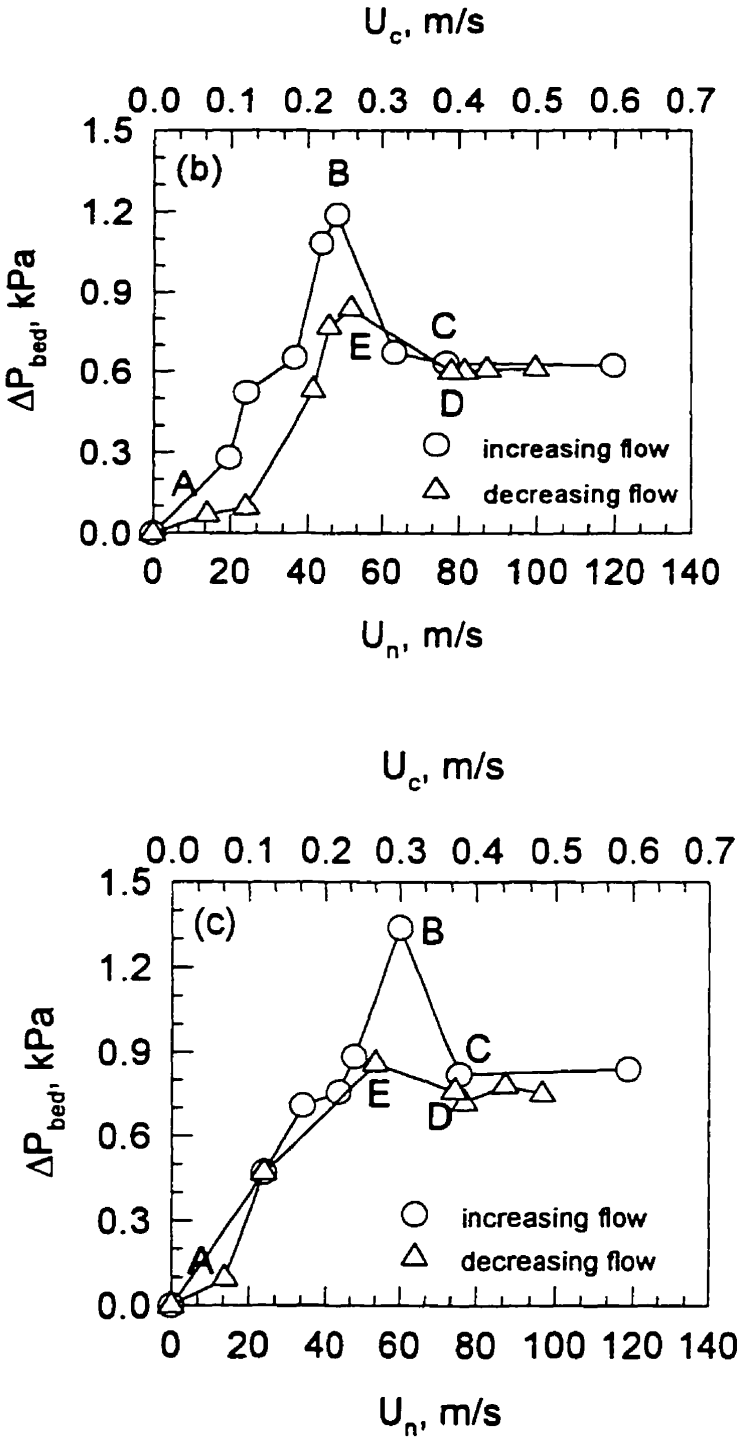

Figure 4.1. Spouting characteristics for rewetted wheat particles, H = 15 cm, D_n = 3 cm, (b) N = 5 rpm, (c) N = 10 rpm. B : peak pressure drop; C : onset of spouting; D : minimum spouting condition; E : spout collapse.

II. Decreasing flow

On decreasing of the gas flowrate the bed pressure drop remains nearly constant and the bed remains in spouting state until point D which represents the minimum spouting condition. A slight reduction of gas velocity causes the spout to collapse and the pressure drop to rise suddenly to point E. Further diminution of flowrate causes pressure drop to decrease steadily along EA. However, the main curve now falls lower than that for the case of increasing flow since the energy required by the gas jet to penetrate the solids is no longer expended during the collapse of the spout [7].

It has been observed that the rotating action of the spouting jet has a great influence on the onset of spouting and hence in lowering the peak pressure drop values by about 30 % as compared to the stationary spouting case. This can be explained by the pulsating action inside the bed which loosens the packed structure and hence facilitates spout evolution.

Observations from the above 3 figures showed that as the air distributor rotational speed is higher the value of air flowrate required to maintain minimum spouting condition is increased. This may be attributed to the fact that the spout has a higher velocity component in the angular direction and hence larger deviation from vertical direction. As a result, more kinetics energy is required to maintain the spouting state. The same phenomenon was also reported by Jumah [5] who studied hydrodynamics in the rotating jet spouted bed.

4.3 Flow Characteristics

Three key hydrodynamic variables, namely, minimum spouting velocity, peak and steady spouting pressure drops, are commonly used to describe flow behavior in spouted bed. In this work experiments were carried out to study these parameters and their relation with spouting medium (air), particle properties as well as equipment parameters. To generalize the discussion and present the experimental results in a useful and compact form empirical equations are developed using dimensional analysis.

4.3.1 Empirical Modelling

It is clear from earlier discussion that the gas-particle dynamics in the RJASB is complicated and difficult to describe analytically. However, some qualitative reasoning based on the observations can be used to determine the dimensionless groups useful in correlating the experimental data. Following the postulations and assumptions made by Jumah [5] and a procedure based on the Buckingham theorem [8], multiple nonlinear regression analysis for evaluation of the correlation coefficients based on Marquardt-Lavenberg method was performed using the SigmaPlot 1.02's Curve Fitter (Jandel Scientific, San Rafael, CA). The following empirical equations for the predictions of minimum spouting velocity, peak and steady spouting pressure drops were then derived :

$$\mathrm{Re}_{msmo} = 0.2448\left(\frac{H}{D_{ce}}\right)^{2.5540}\left(\frac{D_n}{D_{ce}}\right)^{-1.5930} Ar^{0.5502} \tag{4.1}$$

$$\mathrm{Re}_{msn} = 2.0950\left(\frac{H}{D_{ce}}\right)^{0.8196}\left(\frac{D_n}{D_{ce}}\right)^{-0.8316} Ar^{0.5267}\left(\frac{V_\theta}{U_t}\right)^{0.1421} \tag{4.2}$$

$$\frac{\Delta P_M}{\rho_b g H} = 2.3140\left(\frac{H}{D_{ce}}\right)^{0.6139}\left(\frac{D_n}{D_{ce}}\right)^{0.2804} Ar^{0.0450} \tag{4.3}$$

$$\frac{\Delta P_s}{\rho_b g H} = 0.7513\left(\frac{H}{D_{ce}}\right)^{0.7199}\left(\frac{D_n}{D_{ce}}\right)^{0.2827} Ar^{0.1075} \tag{4.4}$$

where

$$V_\theta = 2\pi RN \tag{4.5}$$

in which N is the air distributor rotational speed (revolution per second).

The values of the coefficient of determination, R^2, as well as the standard error and standard deviation for the above results are summarized below in Table 4.1. The ranges of applicability of the correlations proposed are given in Table 4.2.

Table 4.1 Statistical Analysis of the Empirical Correlations

Predicted variable	R^2	Standard deviation	SSE[1]
Re_{msno}	0.986	521.09	1.94×10^6
Re_{msn}	0.988	803.59	2.91×10^7
$\Delta P_M/\rho_b gH$	0.938	0.049	0.058
$\Delta P_S/\rho_b gH$	0.978	0.026	0.017

1. Sum of squares of deviations

Table 4.2 The Range of Applicability of the Correlations for Minimum Spouting Velocity and Pressure Drops.

Dimensionless group	Range
H/D_{ce}	0.250-0.500
D_n/D_{ce}	0.050-0.075
Ar	$7.33 \times 10^5 - 8.52 \times 10^6$
V_θ/U_t	0-0.033

4.3.2 Minimum Spouting Velocity

A spouted bed system is characterized by its minimum flow requirement since there exists a value of minimum air velocity required for spouting. The knowledge of this quantity is important from the viewpoint of design since it is used to specify the blower capacity. Minimum spouting velocity, U_{ms}, depends on the properties of the bed material and spouting agent as well as system geometry. Another added factor in the RJASB is the angular velocity of the air distributor. Again, both the experimental values of jet and column minimum spouting velocities are reported as function of various operating parameters in terms of minimum spouting Reynolds numbers.

Effect of static bed height

Figure 4.2 presents an example of the variation of Re_{ms} with dimensionless bed height for different particles. The data for all particles show that U_{ms} and hence Re_{ms} increases almost linearly as the static bed height is increased. The deeper the bed the larger the amount of air needed to keep the bed at spouting condition and therefore the higher is U_{ms}. Similar observations have been reported also in the literature for spouted bed of other designs [1,3,7].

Effect of air distributor rotational speed

The effect of distributor rotational speed in terms of the dimensionless circumferential velocity, V_θ/U_t, on the corresponding Re_{ms} is presented in Figure 4.3. An increase in rotational speed introduces the resistant forces that tend to deviate the air jet from the vertical direction and thus more flow is required to maintain a stable spouting and consequently higher Re_{ms} values.

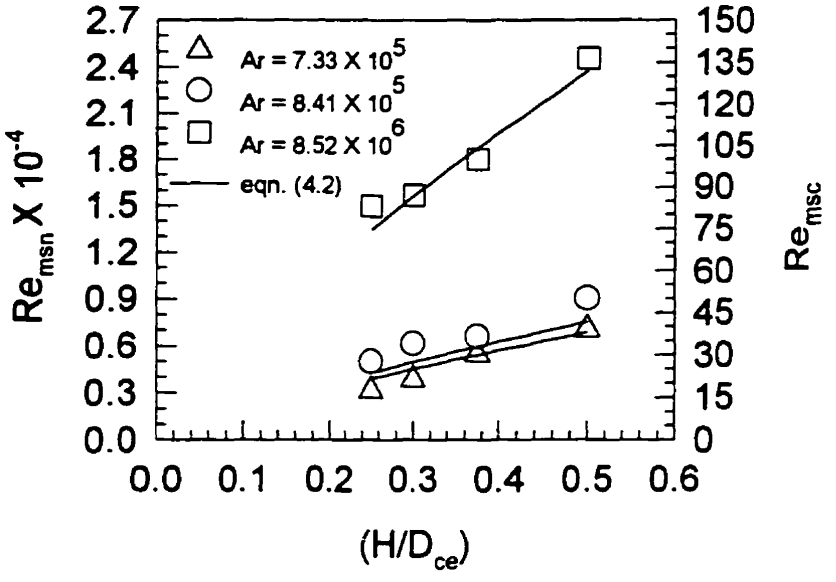

Figure 4.2. Effect of dimensionless bed height on Re_{ms}, D_n/D_{ce} = 0.075, N = 5 rpm.

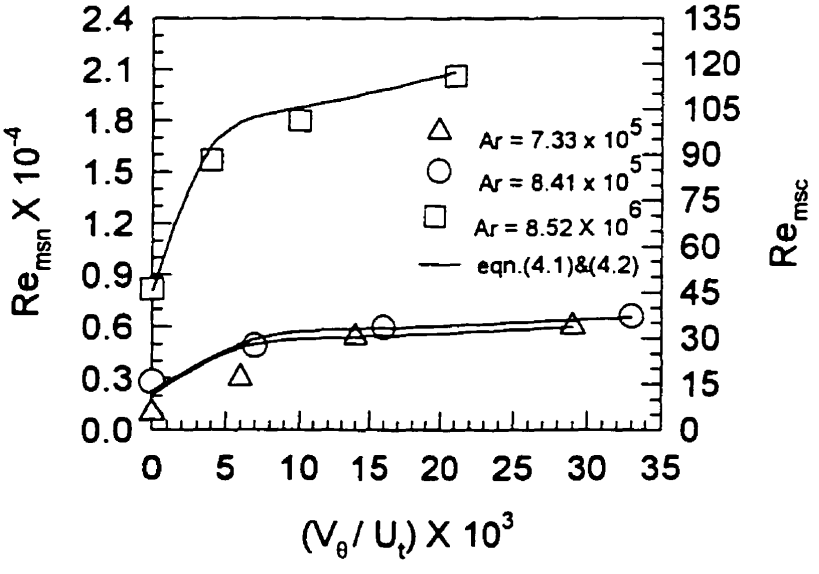

Figure 4.3. Effect of dimensionless circumferential velocity on Re_{ms}, D_n/D_{ce} = 0.075, H/D_{ce} = 0.375.

Effect of particle properties

Additional information on the minimum spouting air flow requirement of RJASB were obtained by examining the effect of particle properties viz. diameter, shape, and density. These properties along with the fluid properties (density, viscosity) are often combined into a single parameter, namely, the Archimedes number which represents the ratio between gravity force and viscous force. The effect of this parameter on Re_{ms} is shown in Figure 4.4 for different values of dimensionless bed height. The main trend is that Re_{ms} increases with Ar. The possible explanation for this phenomenon is that the material with larger Ar, in this case corn, offers more resistance to flow than does a material with lower Ar. Large and dense particles have large mass and respond slowly to the change in fluid flowrate while small and light particles generally follow more closely the changes in fluid motion. Therefore, gravity force is more significant than viscous force for large particles under spouting condition.

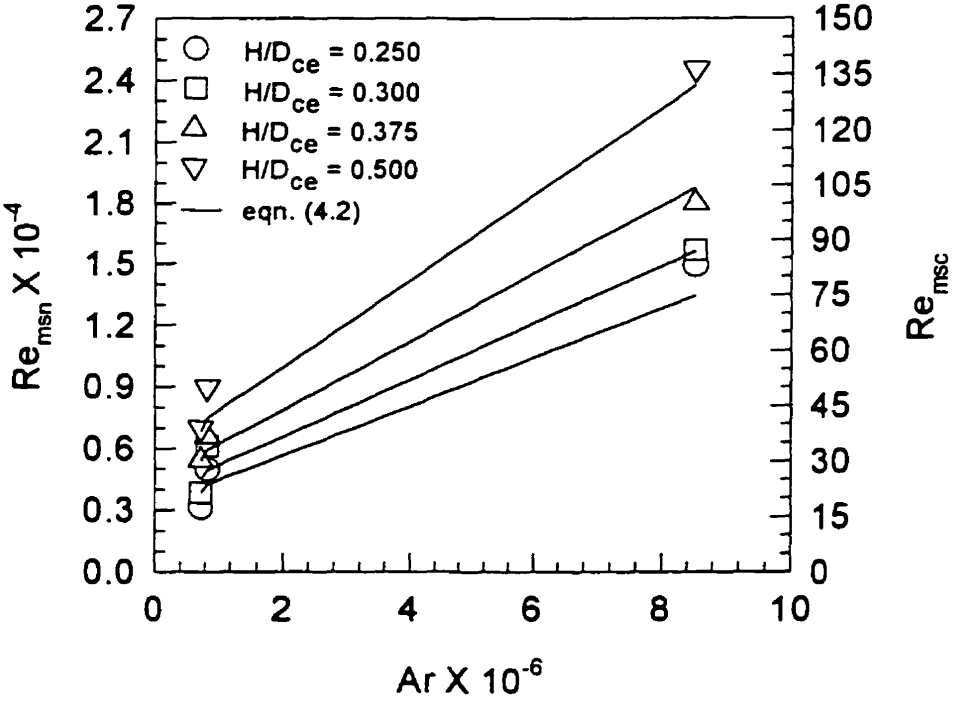

Figure 4.4. Effect of Archimedes number on Re_{ms}, D_n/D_{ce} = 0.075, N = 5 rpm.

Effect of nozzle size

To investigate the effect of nozzle size on the value of minimum spouting velocity, several experiments were performed using two different nozzle diameters for different solid materials and air distributor rotational speeds. The results so obtained are shown in Figure 4.5 as Re_{msc} versus dimensionless circumferential velocity with the dimensionless nozzle diameter as a parameter. As observed from this figure, the value of Re_{msc} increases as the dimensionless nozzle diameter increases. However, as shown in Figure 4.6, the plot of Re_{msn} versus dimensionless circumferential velocity shows an increase in the value of Re_{msn} as the dimensionless nozzle diameter decreases. This is due to the fact that as the nozzle diameter decreases the length basis for nozzle velocity calculation also decreases. This results in higher values of the nozzle (or jet) velocity and hence Re_{msn}. It should be noted that the effect is more pronounced for higher Archimedes number material, i.e., corn in this case.

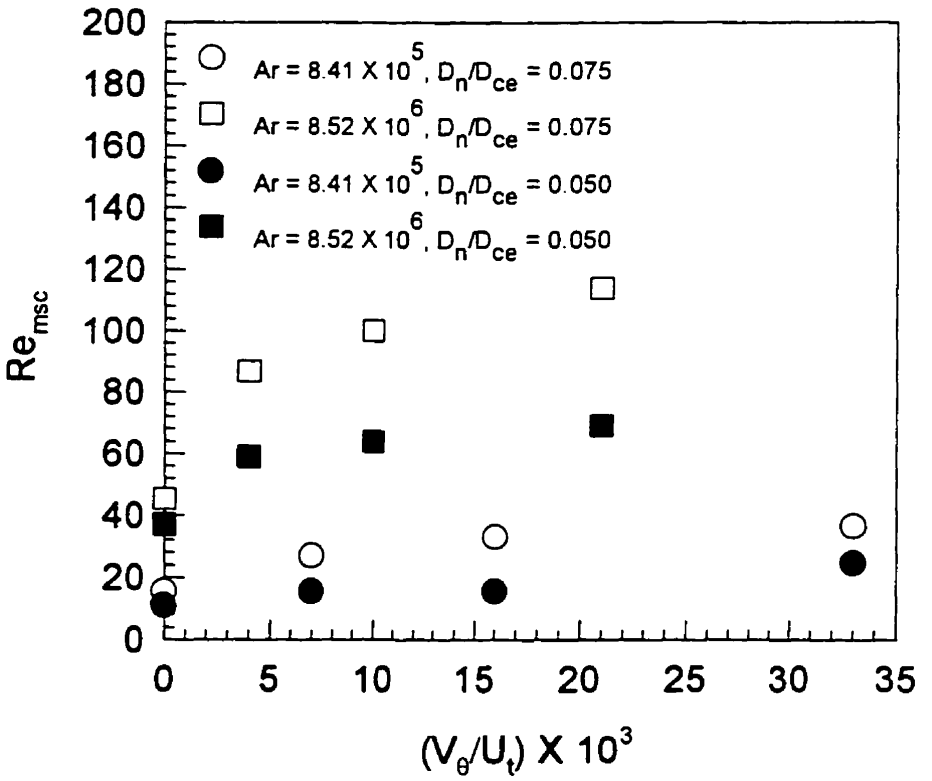

Figure 4.5. Effect of dimensionless nozzle diameter on Re_{msc}, $H/D_{ce} = 0.375$.

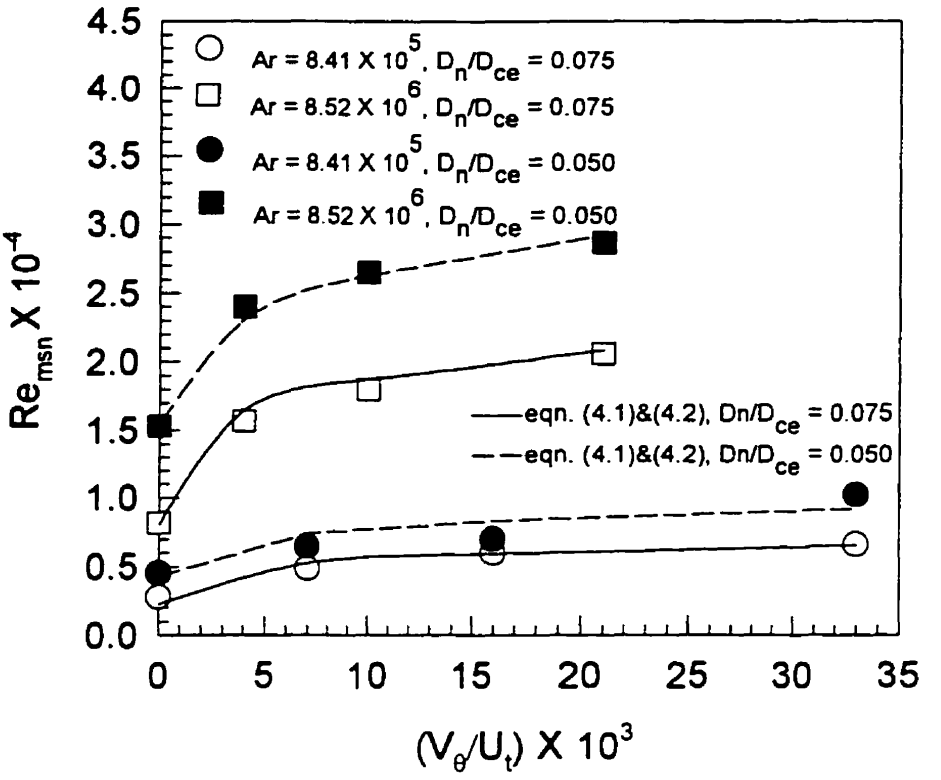

Figure 4.6. Effect of dimensionless nozzle diameter on Re_{msn}, $H/D_{cc} = 0.375$.

From the aforementioned discussion it is thus recommended that larger nozzle size should be used. The use of a smaller nozzle diameter also limits the contact between air and particles because of smaller active spouting area and higher jet velocity.

4.4.3 Pressure Drop

As in conventional spouted bed, two pressure drop values are of practical interest in the design and operation of RJASB, namely, the peak and steady spouting pressure drops. The peak pressure drop (ΔP_M) which is a bed-history dependent variable is encountered when starting up the bed and is used in sizing the air blower system. The steady spouting pressure drop (ΔP_S) corresponds to the nearly constant values beyond the onset of spouting and is useful in estimating the operating power requirements.

Effect of air distributor rotational speed

Figures 4.7 and 4.8 show the effect of air distributor rotational speed on the peak and steady spouting pressure drops, respectively, for two nozzle sizes using corn particles as the test material. These figures show that neither peak nor steady spouting pressure drop is affected by the rotational speed. It is clear, however, that the values of peak pressure drop for stationary distributor (N = 0 rpm) are slightly higher. The lower peak pressure drop values for N > 0 rpm can be attributed to the pulsation and shaking actions introduced by an internal spouting prior to the onset of spouting. This pulsating action helps alleviating the packed condition and thus less energy is required for onset of spouting. Similar behavior was observed also for beds of polystyrene and wheat particles.

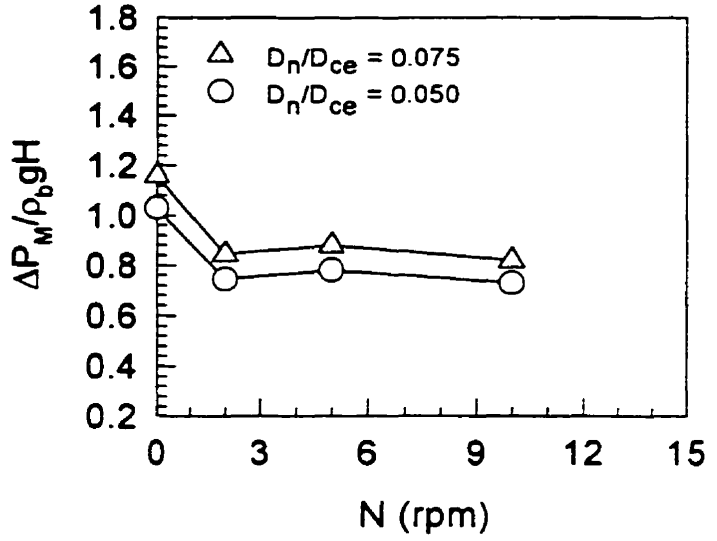

Figure 4.7. Effect of air distributor rotational speed on dimensionless peak pressure drop for corn particles, $H/D_{ce} = 0.375$.

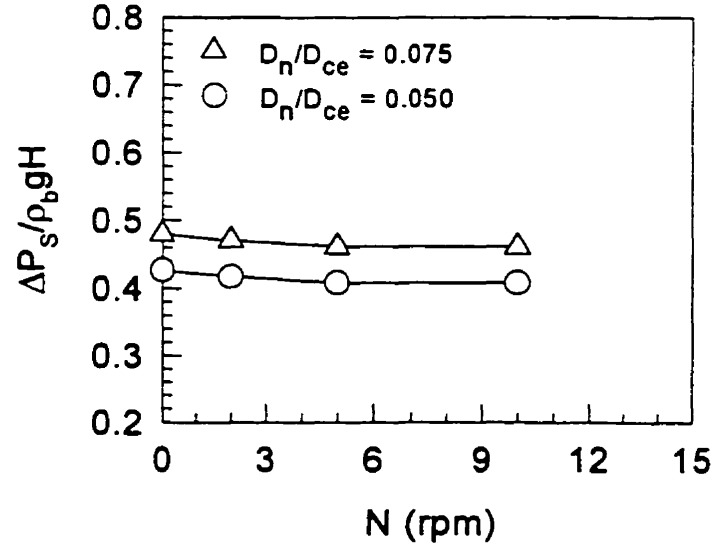

Figure 4.8. Effect of air distributor rotational speed on dimensionless steady spouting pressure drop for corn particles, $H/D_{ce} = 0.375$.

Effect of bed height and nozzle size

In order to analyze the effect of the system geometric parameters of the contactor, the values of dimensionless pressure drops, $\Delta P_M/\rho_b gH$ and $\Delta P_S/\rho_b gH$, are plotted in Figures 4.9 and 4.10, against the dimensionless bed height for different solid materials with the dimensionless nozzle diameter as a parameter. Both *bed* pressure drop values tend to increase with the increase in dimensionless nozzle size. However, the values of *nozzle (or jet)* pressure drops increase significantly with the decrease in nozzle size. The combination of this phenomenon along with that happens in the case of minimum spouting velocity, again, suggested that a larger nozzle diameter should be selected for practical design purpose.

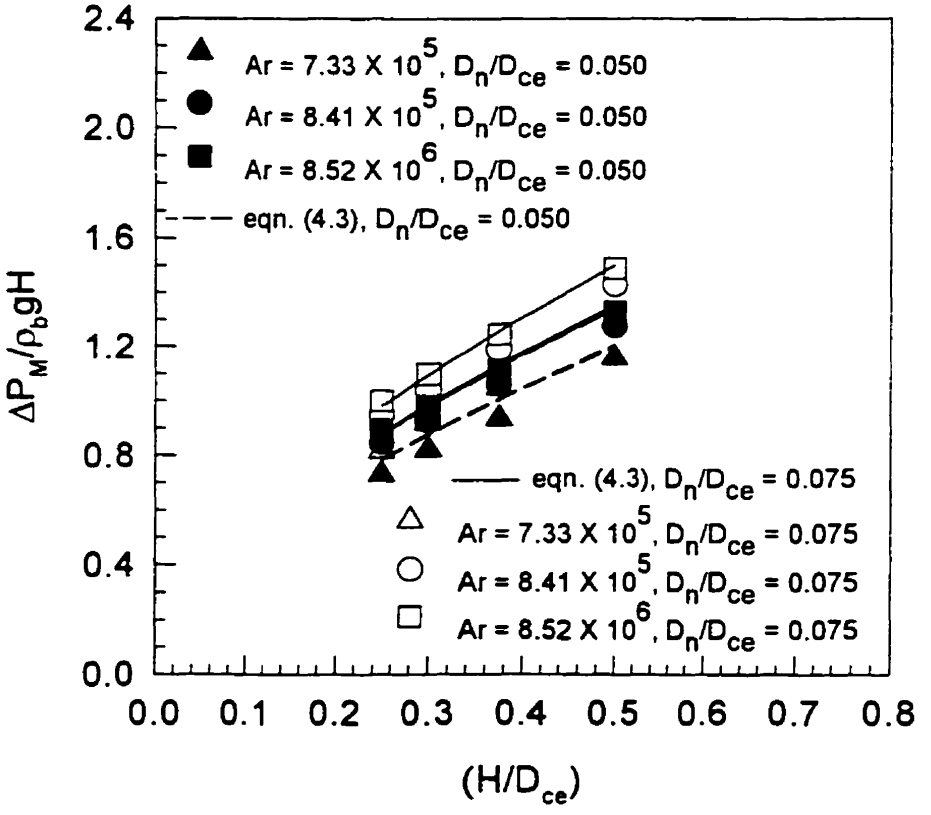

Figure 4.9. Variation of dimensionless peak pressure drop with (H/D_{ce}) and (D_n/D_{ce}) for different solid particles, N = 5 rpm.

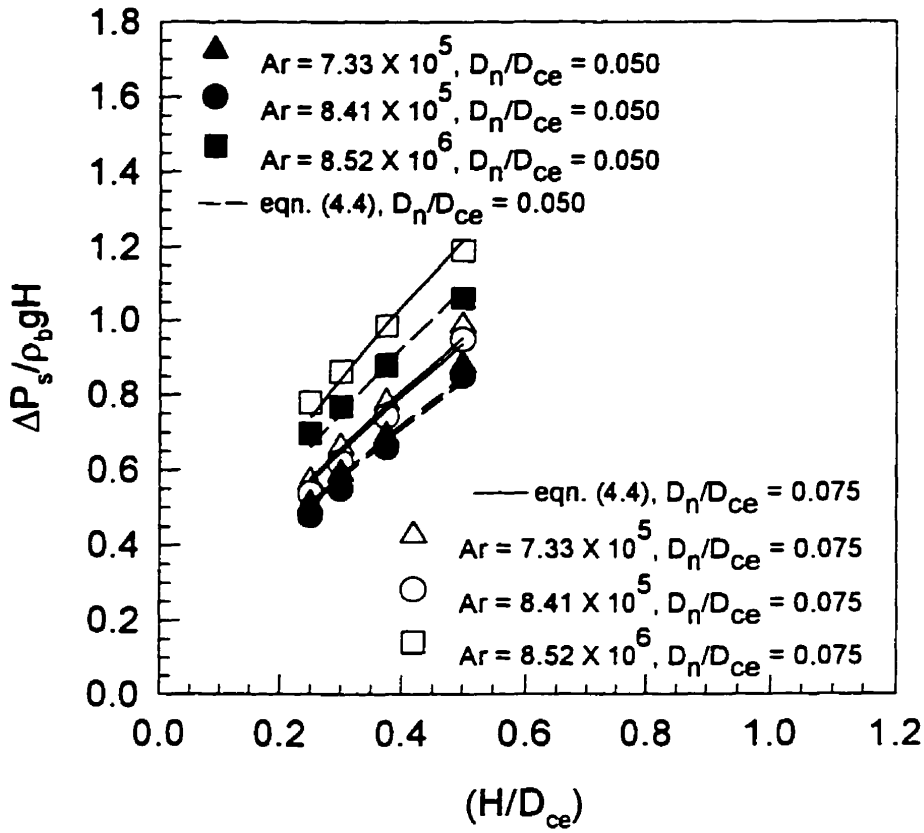

Figure 4.10. Variation of dimensionless steady spouting pressure drop with (H/D_{ce}) and (D_n/D_{ce}) for different solid particles, N = 5 rpm.

4.4 Comparison of Spouting Curves for Wetted/Dried Particulates

In the case when RJASB is utilized as a dryer for materials undergoing falling rate period drying, e.g., some agricultural products, it is interesting to investigate the changes in spouting curves as the process proceeds. For agricultural grains, i.e., wheat in this case, the bed of particles change their own characteristics as drying proceeds due to the changes in density because of the decrease in moisture content and volume because of shrinkage. Figure 4.11 shows two different sets of spouting curves for different stages in the drying of

wheat. The solid curves represent spouting phenomenon for rewetted wheat of high moisture content while dotted curves stand for the spouting behavior for dried wheat at the end of the process. It is clearly seen from this figure that all key hydrodynamic characteristics, i.e., minimum spouting velocity, peak and steady spouting pressure drops, dropped down significantly at the end of the process. This provides an idea that variable drying conditions which could lead to reductions in energy and airflow requirements could be performed.

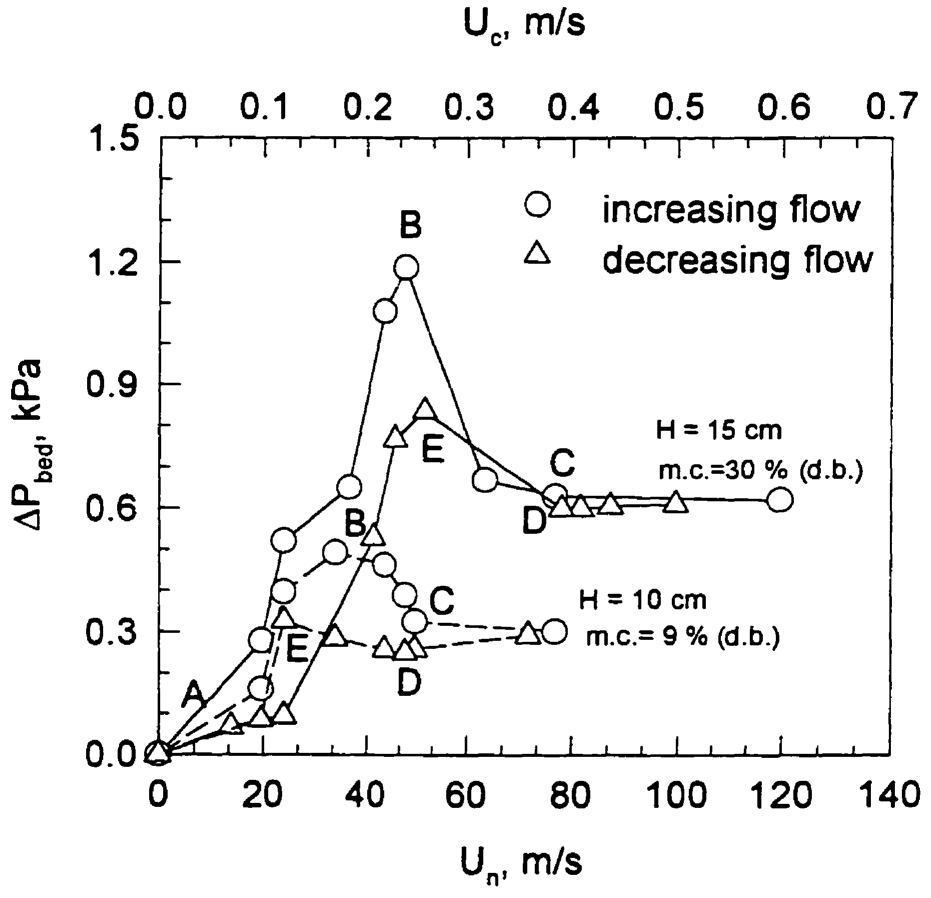

Figure 4.11. Comparison of spouting curves for wetted and dried wheat, H_o = 15 cm, N = 5 rpm, D_n = 3 cm. B : peak pressure drop; C : onset of spouting; D : minimum spouting condition; E : spout collapse.

4.5 Note on Determination of the Fictitious Column Diameter

In order to perform heat/mass transfer calculation in this gas-solid system it is necessary to determine the values of convective heat/mass transfer coefficients which, in turns, requires the calculation of particle Reynolds number. To obtain the particle Reynolds number it is necessary to define the value of the length basis for the determination of superficial velocity used in the calculation. In conventional spouted bed the value of column diameter is normally used as the basis for superficial velocity calculation [7,9]. In the RJASB, however, this figure cannot be employed since not the whole bed is spouted at any instant. Gong et.al. [10] introduced the concept of fictitious column diameter (D_{cf}) in the simulation of wheat drying process in a novel rotating jet spouted bed. The value is, in fact, arbitrarily chosen from the geometric configuration of the spouted bed unit. A more sound theoretical procedure is thus needed in order to determine the value of the fictitious column diameter for general heat/mass transfer calculation.

From visual inspection of spouting phenomenon in RJASB the active spouting region is in the range that Mathur-Gishler Equation can well predict the value of minimum spouting velocity [1]. This equation was then adopted in the calculation of fictitious column diameter. However, some modifications are needed in order to allow this equation to give the value of nozzle minimum spouting velocity instead of column superficial velocity. Multiple nonlinear regression analysis was employed on the experimental data of Mathur and Gishler [11] in order to obtain the values of the new correlation coefficients. The resulting equation becomes :

$$U_{msn} = 74.77\left(\frac{D_p}{D_c}\right)^{1.045}\left(\frac{D_n}{D_c}\right)^{-0.191}\left(\frac{2gH(\rho_s-\rho_g)}{\rho_g}\right)^{0.500} \qquad (4.6)$$

Rearranging for D_c and denoted as D_{cf} yields :

$$D_{cf} = 156.36 \frac{D_p^{1.223}}{D_n^{0.223} U_{msn}^{1.170}} \left(\frac{2gH(\rho_s - \rho_g)}{\rho_g} \right)^{0.585} \tag{4.7}$$

This equation has proved to give the same order of magnitude value as selected by Gong et.al. [10]. Thus it should be employed in any convective heat/mass transfer calculation that requires determination of convective transfer coefficients in the RJASB.

4.6 Conclusions

A novel rotating jet annular spouted bed (RJASB) has been developed for drying particulates in the falling rate period. Experiments were performed to investigate the spouting regimes as well as various key hydrodynamic characteristics in this new gas-solid contactor. Both column superficial and jet velocities were used to demonstrate the spouting phenomenon since the latter seems to be of actual importance in describing of the process. Empirical correlations were developed to predict the values of these parameters for the purpose of design and scale-up.

Comparisons of the spouting behavior for wetted and dried particulates using soft wheat particles as a test material are illustrated and discussed. The results show that the use of a variable drying condition might lead to reductions in energy and airflow requirements as well as to enhancement in the dried product quality.

Nomenclature

D_{cf} fictitious column diameter, m

D_{ce} equivalent cylindrical column diameter, m

D_n nozzle diameter, m

D_p effective particle diameter, m

g gravitational constant, 9.81 m s^{-2}

H static bed height, m

N air distributor rotational speed, rpm

ΔP_{bed} bed pressure drop, kPa

ΔP_M peak pressure drop, kPa

ΔP_S steady spouting pressure drop, kPa

R radius of rotation, m

R^2 coefficient of determination, -

U_c column superficial velocity, m s^{-1}

U_{msc} superficial minimum spouting velocity, m s^{-1}

U_n nozzle minimum spouting velocity, m s^{-1}

U_t particle terminal velocity, m s^{-1}

V_θ circumferential velocity of the air nozzle, m s^{-1}

Greek Letters

μ_g fluid viscosity, kg m^{-1} s^{-1}

ρ_b bulk density, kg m^{-3}

ρ_g fluid density, kg m^{-3}

ρ_s particle density, kg m^{-3}

Subscripts and Superscripts

c	column
ce	equivalent cylindrical column
n	nozzle
ms	minimum spouting condition
msc	column minimum spouting condition
msn	nozzle minimum spouting condition
o	stationary
M	peak
S	steady

Dimensionless Groups

Ar Archimedes number, $\frac{D_p^3 \rho_g (\rho_s - \rho_g) g}{\mu_g^2}$

Re Reynolds number, $\frac{D_p U \rho_g}{\mu_g}$

References

1. Lim, C.J., Grace, J.R., 1987, "Spouted Bed Hydrodynamics in a 0.91 m Diameter Vessel", *Can. J. Chem. Eng.*, 65, pp. 366-372.
2. Passos, M.L., Mujumdar, A.S., Raghavan, V.G.S., 1987, "Spouted Bed for Drying : Principles and Design Considerations", pp.359-398, in A.S. Mujumdar (ed.) *Advances in Drying, Vol. 4*, Hemisphere Publishing Corp., New York.
3. Olazar, M., San Jose, M.J., Aguayo, A.T., Arandes, J.M., Bilbao, J., 1994, "Hydrodynamics of Nearly Flat Base Spouted Beds", *Chem. Eng. J.*, 55, pp. 27-37.

4. Mujumdar, A.S., 1989, "Recent Developments in Spouted Bed Drying", *Keynote Lecture, Transport Processes in Porous Media Conference*, Sao Carlos, S.P., Brazil.
5. Jumah, R.Y., 1995, "Flow and Drying Characteristics of a Rotating Jet Spouted Bed", Ph.D. Thesis, McGill University, Canada.
6. Devahastin, S., Mujumdar, A.S., Raghavan, G.S.V., 1996, "Spouted Beds Research at McGill University", *Proceedings of the International Conference on Food Industry Technology and Energy Applications*", Bangkok, Thailand, pp.22-29.
7. Mathur, K.B., Epstein, N., 1974, "*Spouted Bed*", Academic Press, New York.
8. Buckingham, E., 1914, "On Physically Similar Systems : Illustration of the Use of Dimensional Equations", *Physical Review*, 4, pp. 345-376.
9. Kmiec, A., 1975, "Simultaneous Heat and Mass Transfer in Spouted Beds", *Can. J. Chem. Eng.*, 53, pp.18-24.
10. Gong, Z.X., Devahastin, S., Mujumdar, A.S., 1997, "A Two-Dimensional Finite Element Model for Wheat Drying in a Novel Rotating Jet Spouted Bed", *Drying Technology-An International Journal*, 15(2), pp. 575-592.
11. Mathur, K.B., Gishler, P.E., 1955, "A Technique for Contacting Gases with Coarse Solid Particles", *AIChE. J.*, 1, pp. 157-164.

Chapter 5

Drying Kinetics in the Rotating Jet Annular Spouted Bed : Experimental Results and Mathematical Model

5.1 Introduction

This chapter consists of a detail explanation of a two-dimensional liquid diffusion model for drying of particulates in a Rotating Jet Annular Spouted Bed (RJASB) using rewetted wheat as the test material. The finite element method was employed to solve the set of coupled heat and moisture transfer equations along with appropriate initial and boundary conditions. A new correlation for the effective diffusion coefficient for rewetted wheat was developed using both the experimental as well as numerical results.

5.2 Mathematical Model for Drying of Wheat

Drying of wheat has been studied extensively in the two decades. Becker [1] developed integral solutions for one-dimensional planar, polar and spherical geometries for wheat drying. It was reported that the predicted drying rate by the integral solution is only slightly lower than the experimental results when the wheat particle is modeled as a sphere. Becker and Sallans [2] performed an experimental study of wheat drying in a spouted bed. They modeled the wheat particle as a sphere and obtained a correlation for the drying rate of wheat kernel based on the liquid diffusion theory. They also presented a correlation for the critical grain temperature above which the baking qualities of dried wheat are impaired. Fortes et.al. [3] developed a coupled heat and mass transfer model for wheat drying based on irreversible thermodynamics. In fact, their model is a modified

version of Luikov's model. Theoretically, their model describes more accurately the physics of the heat and mass transfer processes than does a simple liquid diffusion model. However, the applicability of their model is greatly limited due to the fact that the governing equations include many coefficients which are very difficult to determine experimentally. Gong et.al. [4] pointed out the inappropriateness of modelling wheat as a spherical body. These investigators showed the deviation in drying results obtained by using the correlation for effective diffusion coefficient developed by assuming spherical geometry in their two-dimensional liquid diffusion model. Thus, the need for an accurate value of the effective diffusion coefficient becomes crucial. It should be noted that, for simplicity, throughout this work the word "diffusion coefficient" implies "effective diffusion coefficient" unless specified otherwise.

5.3 A Two-Dimensional Liquid Diffusion Model

To model heat and mass transfer processes in a wheat kernel the following assumptions were made:

1. Wheat kernel are uniform in size, homogeneous and isotropic.
2. Moisture transfer within the wheat particle is controlled by liquid diffusion only.
3. Conduction of heat and moisture between bed particles, heat losses and particle shrinkage are negligible.

With the aforementioned assumptions, the governing equations for heat and mass transfer within the wheat kernel are as follows [5] :

$$\frac{\partial X}{\partial t} = \frac{\partial}{\partial x}(D\frac{\partial X}{\partial x}) + \frac{\partial}{\partial y}(D\frac{\partial X}{\partial y}) \qquad (5.1)$$

$$\rho_s c_s \frac{\partial T}{\partial t} = \frac{\partial}{\partial x}(k_s \frac{\partial T}{\partial x}) + \frac{\partial}{\partial y}(k_s \frac{\partial T}{\partial y}) \qquad (5.2)$$

in which

$$D = D_0 \exp(-\frac{E}{RT_{abs}}) \tag{5.3}$$

The initial and boundary conditions are:

Initial condition :

$$\text{at } t = 0, \quad X = X_o \text{ and } T = T_o \tag{5.4}$$

Boundary conditions

for moisture :

$$-D\frac{\partial X}{\partial n} = \frac{V_p m_g}{m_s A_p}(Y - Y_f) \tag{5.5}$$

and for temperature :

$$-k_s \frac{\partial T}{\partial n} = h_T(T - T_f) + \Delta H_{d-v}\frac{m_g \rho_s V_p}{m_s A_p}(Y - Y_f) \tag{5.6}$$

where n is the outward drawn normal vector at the surface.

5.4 Finite Element Formulation

Considering the advantages of the finite element method [6], e.g., there is no need for additional equations to assure continuity across common boundaries of adjacent elements, complex geometries and mesh generation are easily handled, and can easily be generalized

to solve different types of problems, etc., this method was adopted in order to solve the set of coupled equations and the associated initial and boundary conditions.

After spacewise discretization of Eqs. 5.1 and 5.2, subject to convective boundary conditions (Eqn. 5.5 and 5.6), using Galerkin's method [7], the following semi-discrete matrix system is obtained :

$$[C]\{\dot{U}\} + [K]\{U\} = \{F\} \tag{5.7}$$

in which

$$[C] = \sum_{e=1}^{nel} \begin{bmatrix} C_1 & 0 \\ 0 & C_2 \end{bmatrix}^e \tag{5.8}$$

$$[K] = \sum_{e=1}^{nel} \begin{bmatrix} K_1 & 0 \\ 0 & K_2 \end{bmatrix}^e \tag{5.9}$$

$$[U] = \sum_{e=1}^{nel} \begin{bmatrix} X \\ T \end{bmatrix}^e \tag{5.10}$$

$$[F] = \sum_{e=1}^{nel} \begin{bmatrix} F_1 \\ F_2 \end{bmatrix}^e \tag{5.11}$$

In the preceding equations, *nel* is the total number of elements; the superposed dot denotes differentiation with respect to time; the superscript *e* designates an element; C_1, C_2, K_1 and K_2 are submatrices; F_1 and F_2 are subvectors. The coefficients in the submatrices and subvectors are calculated according to the following equations:

$$C_1^{IJ} = \int_{\Omega^e} \rho_s c_s N_I N_J \, dxdydz \tag{5.12}$$

$$C_2^{IJ} = \int_{\Omega^e} N_I N_J \, dxdydz \tag{5.13}$$

$$K_1^{IJ} = \int_{\Omega^e} D\left(\frac{\partial N_I}{\partial x}\frac{\partial N_J}{\partial x} + \frac{\partial N_I}{\partial y}\frac{\partial N_J}{\partial y} + \frac{\partial N_I}{\partial z}\frac{\partial N_J}{\partial z}\right) dxdydz \qquad (5.14)$$

$$K_2^{IJ} = \int_{\Omega^e} k\left(\frac{\partial N_I}{\partial x}\frac{\partial N_J}{\partial x} + \frac{\partial N_I}{\partial y}\frac{\partial N_J}{\partial y} + \frac{\partial N_I}{\partial z}\frac{\partial N_J}{\partial z}\right)dxdydz + \int_{\Gamma^e} h_T N_I N_J d\Gamma \qquad (5.15)$$

$$F_1^I = \int_{\Gamma^e} h_m (Y - Y_{en}) N_I d\Gamma \qquad (5.16)$$

$$F_2^I = \int_{\Gamma^e} [h_T T_{en} + \Delta H h_m (Y - Y_{en})] N_I d\Gamma \qquad (5.17)$$

Discretization of the time derivative in Eq. 5.7 is achieved with backward Euler scheme :

$$[C + \Delta t K]\{U_{t+\Delta t}\} = [C]\{U_t\} + \{F\} \qquad (5.18)$$

Based on the procedure described above, a two-dimensional finite element computer code was written in FORTRAN 77. Using this computer code simulations of rewetted wheat drying in the novel RJASB were carried out.

5.5 Results and Discussion

The cross-section of a typical soft wheat kernel is shown schematically in Figure 5.1. When the wheat particle is dried in the rotating jet annular spouted bed, the surface of the wheat is exposed to hot air and subjected to convective heat and mass transfer.

The particles in the rotating jet annular spouted bed have been shown to be well mixed so that it can be assumed that the surface of the wheat is subjected to uniform convective heat and mass transfer. Therefore, the convective transfer coefficients and the temperature as well as the humidity of the drying air are taken to be as uniform at every location on the wheat surface.

According to the derivation of the boundary conditions for a grain particle in the spouted bed [5] T_f and Y_f are the temperature and humidity of the inlet hot air of the spouted bed and h_T is calculated using the following correlation [8]:

$$Nu = \frac{h_T D_p}{k_g} = 0.897\,\mathrm{Re}^{0.464}\,\mathrm{Pr}^{0.333}\,Ar^{0.116}(H/D_{p_e})^{-1.19}\phi^{2.261} \qquad (5.19)$$

The superficial velocity used to calculate the Reynolds number in (5.19) is based on a fictitious column diameter value calculated according to the procedure given in Chapter 4. It should be noted that since this correlation was developed by assuming the particle to be spherical, the diameter substituted must be an equivalent spherical diameter in order to obtain the Nusselt number. The effective particle diameter is then used to calculate the value of heat transfer coefficient.

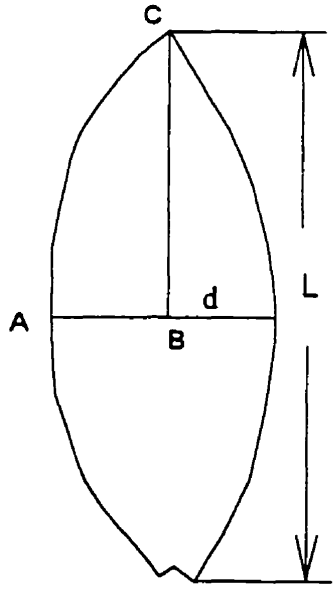

Figure 5.1. Schematic cross-section of a typical soft wheat kernel.

5.5.1 Experimental Validation of the Numerical Model

The numerical model was first validated by comparing the computed results assuming wheat as a one-dimensional spherical body with the experimental data for wheat drying in the rotating jet annular spouted bed apparatus.

The relevant experimental parameters used for model validation are listed in Table 5.1. The transport and equilibrium properties of soft wheat are listed in Table 5.2. The thermodynamic and transport properties of air-water system are listed in Table 5.3.

Table 5.1 Experimental Parameters Used for Model Validation

Parameter	Value	Unit
Y_{gi}	0.008	kg/kg
T_o	15.0	°C
m_s	6.0	kg
H	0.15	m
X_0	0.30	kg/kg
A_p	2.40×10^{-5}	m^2
V_p	1.10×10^{-8}	m^3
ρ_s	1182.0	kg/m^3
d	0.0035	m
L	0.00586	m
ϕ	0.616	-

Table 5.2 Transport and Equilibrium Properties of Soft Wheat

Property	Expression	Reference
D	$D_1 = 0.0198\exp(-6155/T_{abs})$	[9]
k_s	$k_s = [0.117 - 0.003808(X + X_e)]/[1.0 - (X - X_e)]$	[3]
C_s	$C_s = [1396 + 2688(X + X_e)]/[1 - (X + X_e)]$	[3]
RH	$RH = 1 - \exp[-c_1(100X_e)^{c_2}(T + c_3)]$ $c_1 = 2.3008 \times 10^{-5}$, $c_2 = 2.2857$, $c_3 = 55.82$	[10]
ΔH_{d-v}	$\Delta H_{d-v} = R_v T_{abs}^2[(6887/T_{abs}^2) -$ $(5.31/T_{abs}) + (1 - RH)c_1(100X_e)^{c_2}/RH]$	[10]

Table 5.3 Thermodynamic and Transport Properties of Air-Vapor Systems [11,12]

Property	Expression
P_v	$P_v = 100\exp[27.0214 - (6887/T_{abs}) - 5.32\ln(T_{abs}/273.16)]$
Y	$Y = 0.622RH\,P_v/(P - RH\,P_v)$
c_{ps}	$c_{ps} = 1.00926 \times 10^3 - 4.0403 \times 10^{-2}T + 6.1759 \times 10^{-4}T^2 - 4.097 \times 10^{-7}T^3$
k_g	$k_g = 2.425 \times 10^{-2} - 7.889 \times 10^{-5}T - 1.790 \times 10^{-8}T^2 - 8.570 \times 10^{-12}T^3$
ρ_g	$\rho_g = PM_g/(RT_{abs})$
μ_g	$\mu_g = 1.691 \times 10^{-5} + 4.984 \times 10^{-8}T - 3.187 \times 10^{-11}T^2 + 1.319 \times 10^{-14}T^3$
c_{pv}	$c_{pv} = 1.883 - 1.6737 \times 10^{-4}T + 8.4386 \times 10^{-7}T^2 - 2.6966 \times 10^{-10}T^3$
c_{pw}	$c_{pw} = 2.8223 + 1.1828 \times 10^{-2}T - 3.5043 \times 10^{-5}T^2 + 3.601 \times 10^{-8}T^3$

First, a simple spherical geometry was chosen to approximate the wheat kernel. For an air temperature of 63 °C and a mass flow rate of hot air of 0.087kg/s, grid dependence tests showed that the maximum difference between the predicted average moisture content during

the drying process was less than 0.17 % between numerical runs using 20 elements with a time step of 20 second and 80 elements with a time step of 5 seconds, while the maximum difference was less than 0.05% when using 40 elements with a time step of 10 second and 80 elements with a time of 5 seconds. Considering both accuracy and computing time 40 elements with a time step of 10 seconds were utilized.

Figure 5.2 presents a comparison of the drying curves between the model predictions and the experimental results for an inlet air flow rate of 0.087 kg/s and the inlet air temperatures of 63 °C and 79 °C. In this figure the solid line represents the numerical results and the upward open triangle and the downward open triangle represent the experimental results for the inlet air temperature of 63 °C and 79 °C, respectively. It is seen from this figure that there is an excellent agreement between the numerical predictions and the experimental results despite the numerous simplifying assumptions.

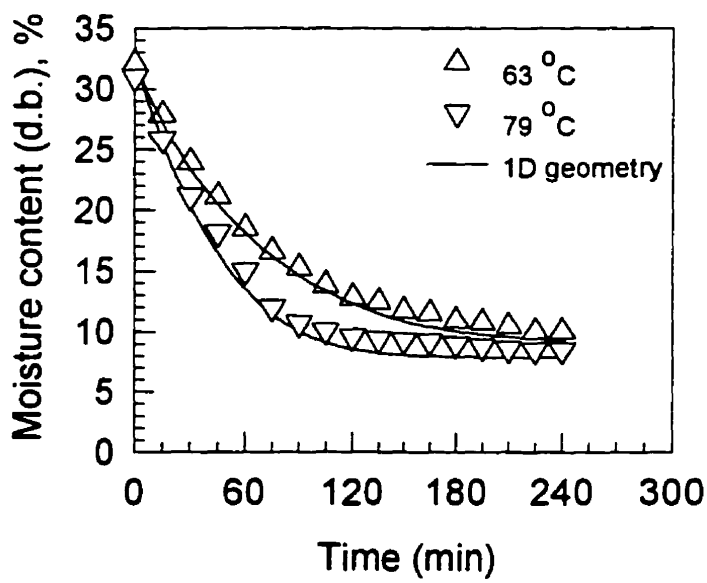

Figure 5.2. Comparison of the numerical predictions assuming spherical geometry with the experimental results. N = 5 rpm, D_n = 3 cm, H = 15 cm, U_c = 0.64 m/s, $X_0 \cong 0.30$ kg/kg

5.5.2 Effect of Modelling Geometry

As pointed out by Gong et.al [4] the assumed geometry has a strong effect on the results obtained. Two geometries, one-dimensional spherical and a fully two-dimensional geometry, were selected to illustrate this effect. The wheat kernel cross-section shown in Figure 5.1 is assumed to be an axi-symmetric plane. Due to symmetry only a quarter can be used in the computation. The finite element meshes of the axi-symmetric geometry are shown in Figure 5.3. For the two geometries, wheat kernel drying rates with an inlet air temperature of 63 ^{0}C and an air flowrate of 0.087 kg/s were computed. Figure 5.4 displays the effect of the modelling geometry on the drying curves. In this figure the solid and dashed line represent results computed for the spherical and two-dimensional geometries, respectively. Clearly the simulation assuming spherical geometry (1D) yields better agreement with the experimental data. This is because the effective diffusivity value used in the simulation was obtained by assuming spherical geometry of wheat kernel.

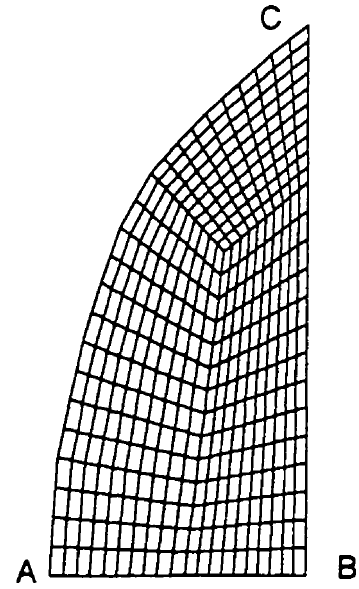

Figure 5.3. Finite element meshes for axi-symmetric geometry

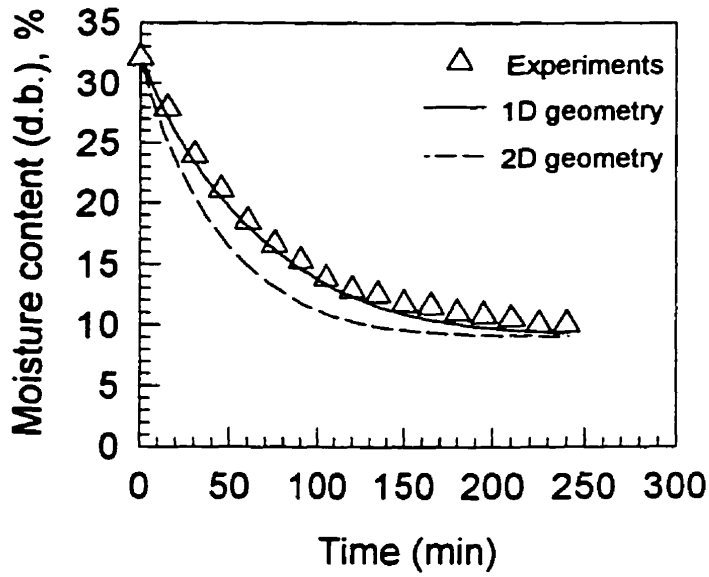

Figure 5.4. Effect of modelling geometry on predicted drying curves.
H = 15 cm, D_n = 3 cm, U_c = 0.64 m/s, T_i = 63 °C, N = 5 rpm, $X_o \cong 0.32$ kg/kg

5.5.3 A New Two-Dimensional Based Diffusion Coefficient

Based on both the experimental and numerical results, a two-dimensional based effective diffusion coefficient has been developed assuming an Arrhenius type relationship for temperature dependence :

$$D_2 = 0.0105 \exp(-6155/T_{abs}) \qquad (5.20)$$

A moisture-independent nature of the diffusion coefficient is also reported by another investigator who studied wheat drying process [2].

5.5.4 Comparison Between Numerical Predictions and Experimental Results

Two sets of results are compared in Figure 5.5 showing the effect of inlet air temperature on the average moisture removal rate. All the parameters used for the two cases were the same except for the inlet air temperatures.

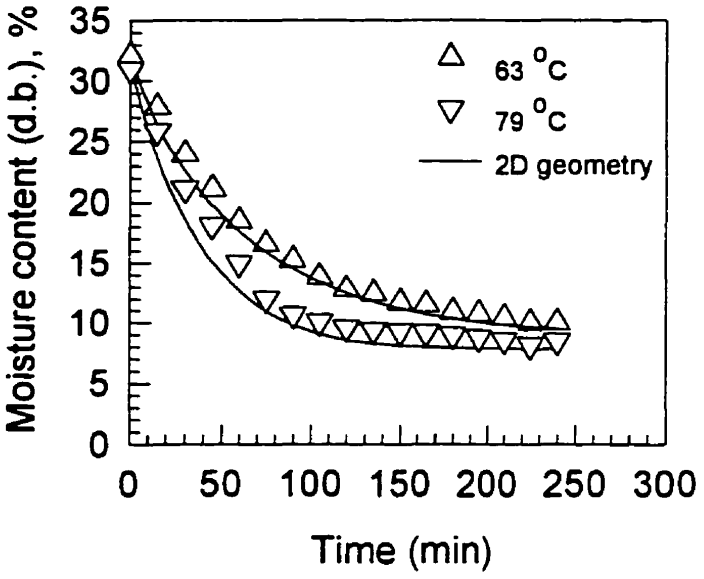

Figure 5.5. Effect of inlet air temperature on drying curves : Comparison between experimental and numerical results

N = 5 rpm, H = 15 cm, D_n = 3 cm, U_c = 0.64 m/s, $X_0 \cong 0.30$ kg/kg

It can be seen also from this figure that an increase of the inlet air temperature can greatly accelerate the moisture removal rate. However, the inlet air temperature cannot be increased indefinitely since there exists a critical temperature above which the baking qualities are thermally injured [2]. Also shown in Figure 5.6 is the effect of inlet air temperature on the kernel surface temperature. It is obvious that the temperature of the drying air has a strong effect on the kernel temperature. Thus, it is important to pay attention to this parameter in order to avoid overheating of the dried product. It is seen

from these two figures that the agreement between numerical and experimental results obtained is good. The small discrepancy between the predicted and observed temperatures is attributed to the uncertain measurement of the particle surface temperature, and the simplifying assumptions made in the development of the model, e.g., neglecting heat losses and errors in estimating air-water system properties. The same phenomenon is also reported by Jumah et.al. [5] who dried yellow dent corn in a rotating jet spouted bed of a different design.

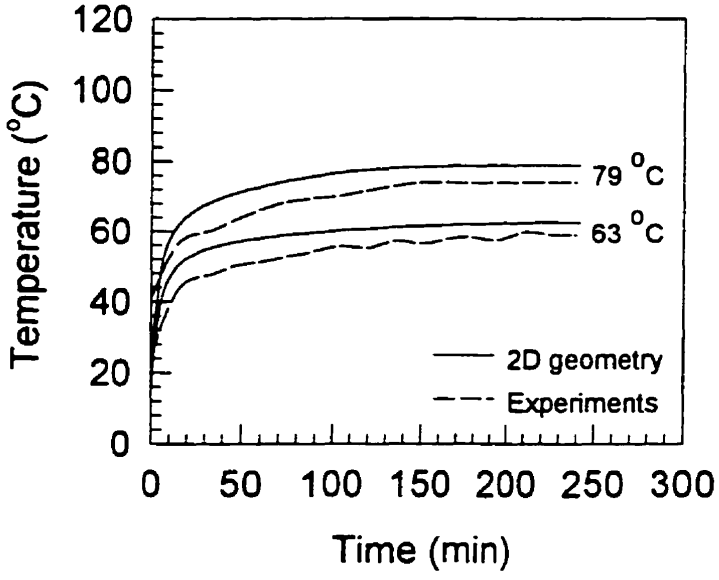

Figure 5.6. Effect of inlet air temperature on kernel surface temperature :
Comparison between experimental and numerical results
N = 5 rpm, H = 15 cm, D_n = 3 cm, U_c = 0.64 m/s, $X_0 \cong 0.30$ kg/kg

Figure 5.7 presents the effect of initial bed height on the drying curves. It is seen from this figure that the drying rate decreases slightly with the increase in static bed height. A reduction in bed height results in a shorter particle cycle time and thus higher temperature gradients inside the particle, higher surface temperature and hence higher diffusivity and therefore drying rates. This phenomenon is shown in Figure 5.8 for the variation of surface temperature with time.

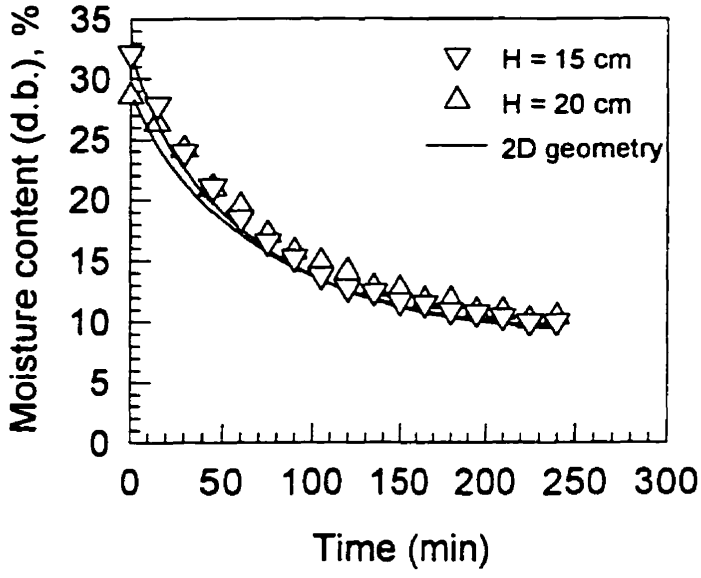

Figure 5.7. Effect of initial bed height on drying curves :
Comparison between experimental and numerical results
$N = 5$ rpm, $U_c = 0.64$ m/s, $T_i = 63$ °C, $D_n = 3$ cm, $X_o \cong 0.30$ kg/kg

Shorter bed height also leads to a lower average vapor concentration in the gas phase, and therefore, the mean driving force for heat and mass transfer increases resulting in an increased drying rate.

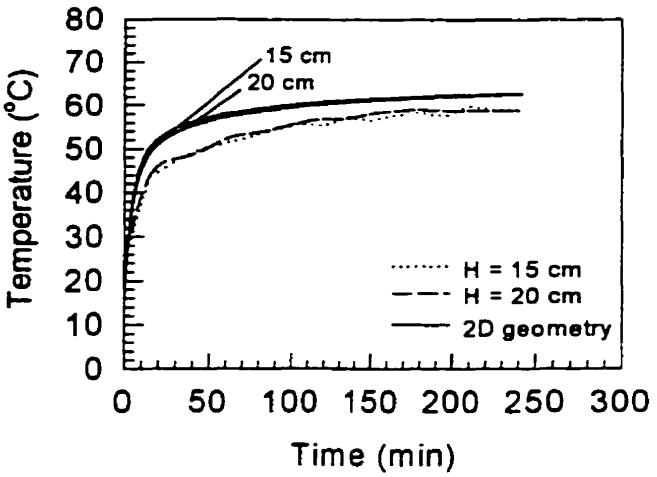

Figure 5.8. Effect of initial bed height on kernel surface temperature : Comparison between experimental and numerical results

N = 5 rpm, U_c = 0.64 m/s, T_i = 63 °C, D_n = 3 cm, $X_o \cong 0.30$ kg/kg

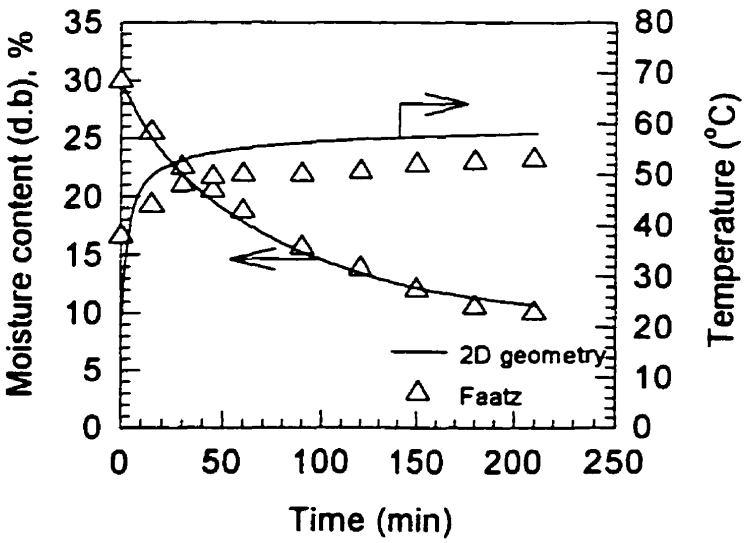

Figure 5.9. Comparison between Faatz's and simulated results

N = 4 rpm, U_c = 0.45 m/s, D_n = 3 cm, H = 15 cm, T_i = 58 °C, $X_o \cong 0.30$ kg/kg

Figure 5.9 shows the comparison between the experimental results of drying wheat in a rotating jet spouted bed [13] and simulated one. It can be seen that the agreement between these two data set is good. Thus further confirmed the validity of the obtained result.

5.6 Concluding Remarks

Choice of the physical geometry of the kernel used for simplified computation has significant influence on the predicted heat/mass transfer rates. Since the value of the diffusion coefficient is obtained by assuming a certain geometry it is thus important to choose the model geometry correctly. This is especially important when one wishes to model the transient thermal and moisture distribution within the kernel accurately so that quality parameters may be modelled in later work.

In this work, a two-dimensional liquid diffusion model was developed to simulate the heat and mass transfer processes in the falling rate period drying of cereal grains in a novel rotating jet annular spouted bed. Rewetted wheat was used as the test material. A correlation for the effective diffusion coefficient was developed using both the experimental and numerical results. The result obtained was verified and found to be in good agreement with the experimental results.

It should be pointed out that the result obtained can be adapted to other processes which require more accurate description of the thermal and moisture distribution in the grain, e.g., stress-cracking analysis, determination of moisture distribution inside a kernel, etc.

Nomenclature

A_p particle surface area, m^2

c_p specific heat, $J\ kg^{-1}K^{-1}$

c_s specific heat of wheat, $J\ kg^{-1}K^{-1}$

D diffusion coefficient, $m^2\ s^{-1}$

D_0 diffusion coefficient at reference temperature, $m^2\ s^{-1}$

D_{p_e} equivalent spherical diameter, m

d characteristic particle diameter, m

E activation energy, kJ

g gravitational constant, 9.81 $m\ s^{-2}$

H bed height, m

h_T convective heat transfer coefficient, $W\ m^{-2}K^{-1}$

ΔH_{d-v} heat of desorption-vaporization of water, $kJ\ kg^{-1}$

k thermal conductivity, $W\ m^{-1}K^{-1}$

k_s thermal conductivity of wheat, $W\ m^{-1}K^{-1}$

L characteristic particle dimension, m

M_w molar mass of water, $kg\ mol^{-1}$

m_g mass flow rate of dry air, $kg\ s^{-1}$

m_s mass of dry solid in bed, kg

N shape function

n outward normal of boundary

P_v vapor pressure of pure water, Pa

R universal gas constant, 8.314 $J\ mol^{-1}K^{-1}$

RH relative humidity, -

R_v $R/M_w = 462\ J\ kg^{-1}K^{-1}$

T temperature, °C

T_{abs} absolute temperature, K

T_f ambient temperature, °C

t	time, s
Δt	time step, s
U	air superficial velocity, m s^{-1}
V_p	particle volume, m^3
X	free moisture content, kg/kg (d.b.), -
Y	absolute air humidity, kg water vapor/kg dry air
Y_f	absolute ambient humidity, kg water vapor/kg dry air
Y_{gi}	absolute ambient humidity of the inlet air, kg water vapor/kg dry air
x,y,z	coordinates, m

Greek Letters

ρ	density, kg m^{-3}
ρ_s	density of wheat, kg m^{-3}
Γ, Γ^e	boundary which subjected to convective transfer
Ω^e	integration domain of an element
ϕ	sphericity, -
μ	viscosity, kg $m^{-1}s^{-1}$

Subscripts and Superscripts

1	one-dimensional geometry
2	two-dimensional geometry
e	equilibrium
o	initial value
g	gas
i	inlet
I, J	element node number
p	particle

s solid

v vapor

w water

Dimensionless Groups

Ar Archimedes number, $\frac{D_p^3 \rho_g (\rho_s - \rho_g) g}{\mu_g^2}$

Nu Nusselt number, $\frac{h_T D_p}{k_g}$

Pr Prandtl number, $\frac{c_{pg} \mu_g}{k_g}$

Re Reynolds number, $\frac{D_p U \rho_g}{\mu_g}$

References

1. Becker, H.A., 1959, "A Study of Diffusion in Solids of Arbitrary Shapes, with Application to the Drying of the Wheat Kernel", *J. Appl. Poly. Sci.*, 1, pp.212-226.
2. Becker H.A., Sallans, H.R., 1960, "Drying Wheat in a Spouted Bed : On the Continuous Moisture Diffusion Controlled Drying of Solid Particles in a Well-Mixed, Isothermal Bed", *Chem. Eng. Sci.*, 13, pp.97-112.
3. Fortes, M., Okos, M.R., Barrett, Jr., J.R., "Heat and Mass Transfer Analysis of Intra-Kernel Wheat Drying and Rewetting", *J. Argic. Engng. Res.*, 26, pp. 109-125.
4. Gong, Z.X., Devahastin, S., Mujumdar, A.S., 1997, "A Two-Dimensional Finite Element Model for Wheat Drying in a Novel Rotating Jet Spouted Bed", *Drying Technology-An International Journal*, 15(2), pp. 575-592.
5. Jumah, R.Y., Mujumdar, A.S., Raghavan, G.S.V., 1996, "A Mathematical Model for Constant and Intermittent Batch Drying of Grains in a Novel Rotating Jet Spouted Bed", *Drying Technology-An International Journal*, 14, pp.765-802.

6. Oliveira, L.S., Haghighi, K., 1997, "Finite Element Modelling of Grain Drying", pp. 309-338, in I. Turner and A.S. Mujumdar (eds.) *Mathematical Modelling and Numerical Technique in Drying Technology*, Marcel Dekker, Inc., New York.
7. Zienkiewicz, O.C., Taylor, R.L., 1989, "*The Finite Element Method*', *Vol.1*, 4th ed., McGraw-Hill Inc., London.
8. Kmiec, A., 1975, "Simultaneous Heat and Mass Transfer in Spouted Beds", *Can. J. Chem. Eng.*, 53, pp.18-24.
9. Brooker, D.B., Bakker-Arkema, F.W., Hall, C.W., 1992, "*Drying and Storage of Grains and Oilseeds*, Van Nostrand Reinhold, New York.
10. Zahed, A.H., Epstein, N., 1992, "Batch and Continuous Spouted Bed Drying of Cereal Grains : The Thermal Equilibrium Model", *Can. J. Chem. Eng.*, 70, pp.945-953.
11. Pakowski, Z., Bartczak, Z., Strumillo, C., Stenstrom, S., 1992, "Evaluation of Equations Approximating Thermodynamic and Transport Properties of Water, Steam and Air for Use in CAD of Drying Processes", *Drying Technology-An International Journal*, 9, pp. 753-773.
12. Mujumdar A.S., 1995, "*Handbook of Industrial Drying*, Appendix", 2nd ed., Marcel Dekker, Inc., New York.
13. Faatz, P., 1995, "Experimental Study of Drying Characteristics of Wheat in a Rotating Jet Spouted Bed", Unpublished Data, Chemical Engineering Department, McGill University, Canada.

Chapter 6

Conclusions

The following conclusions are made based on this investigation :

- The key hydrodynamic characteristics, e.g., minimum spouting velocity, peak and steady spouting pressure drops were measured using polystyrene, corn and wheat as the test materials. Empirical correlations were developed which are useful in the design and scale-up of RJASB. They include effects of bed height, nozzle diameter, air distributor rotational speed as well as particle characteristics.

- The air distributor rotational speed has appreciable effect on the value of minimum spouting velocity. The effect on peak pressure drop is dominant only when shifting from stationary spouting to rotating spouting regime while the effect is negligible on the value of steady spouting pressure drop for the whole range of study.

- Drying tests in the RJASB were conducted using rewetted wheat as the test material. Only wheat was chosen because it is nonspherical and dries only in the falling rate period. Effects of spouting air temperature as well as bed height were determined experimentally. A finite element solution to the two-dimensional liquid diffusion equation was obtained with an accurate physical description of the wheat kernel and compared with the conventional one-dimensional model assuming the wheat kernel to be spherical. A new effective liquid diffusivity correlation was obtained for rewetted wheat using the experimental data.

Recommendations

- Flow characteristics of the RJASB system using two (or four) rotating inlet air nozzles within a large diameter column should be investigated. The distance of the nozzles from the center of the vessel need not be the same. This allows use of larger column diameters and still avoid any dead areas.

- Experimental studies on drying are needed using freshly harvested grains as well as other nonagricultural particulate solids.

- Once two-dimensional effective liquid diffusivities are obtained simulations could be carried out for intermittent spouting and heating to optimize energy and quality of dried products

Appendix I

A Colorimetric Technique to Quantify Wheat Grain Damage During Drying

A.1 Introduction

Quality is one of the most important parameters to be considered in selection and operation of the drying process. During grain drying some damage, both thermal and mechanical, can occur. To minimize such damage it is important to be able to determine the damage quantitatively under various operating conditions. The usual method of visual inspection and reporting the damage levels as percentage by weight is time-consuming, inaccurate and does not account for the fact that damage may occur on a continuous scale [1].

Several methods have been employed to determine grain damage. Visual inspection, though simplest, has some shortcomings. Schmidt et.al. [2] reported a study in which the precision of estimating mechanical damage of corn was investigated. Experimental results showed considerable variation among damage observed. Main sources of variation in sample damage estimates were observer differences, sampling differences and the inability of observers to repeat their determination of damage. Thus, a method which provides systematic procedure of determining such damage is needed.

A colorimetric technique which employs the technique of spectrophotometry was originally developed by Chowdhury and Buchele [3]. This technique consists of staining the damaged parts of grains in a Fast Green FCF dye; the dye reacts only with the exposed internal tissue of the grains. Excess dye is rinsed off with distilled water and the sample is then placed in a mild sodium hydroxide solution which dissolves the dye adhering only to

the damaged grains. The percentage transmittance or absorbance of the solution is then measured using a spectrophotometer. It is obvious that the greater the damage level in the sample, the greater the absorbance.

In this study [4], the calibration curves were constructed based on artificial "half-cut" damage of wheat. The percent damage of wheat resulting from the spouting process is then reported based on the "half-cut" scale. This work was motivated by the need to examine the quality of grains dried in the novel dryer as far as mechanical damage is concerned. It should be noted that the experimental results presented here are for wheat drying in a novel rotating-impinging jet spouted bed which, in fact, should produce the same order of damage as will be in RJASB.

A.2 Material and Methods

A.2.1 Material

Soft Spring wheat kernels were used as the test material. According to Geldart's specification [5], wheat is classified as a class D (spoutable, large and dense) particle. Selected properties of wheat are summarized in Table 3.1-3.3.

A.2.2 Experimental method

A.2.2.1 The colorimetric method

The colorimetric method consists of scanning for the absorbance peak of the Fast Green FCF dye in a dilute aqueous solution of sodium hydroxide (Figure A.1). The wavelength at which peak absorbance occurs (λ = 607 nm) is then used to adjust the reading wavelength of the spectrophotometer. A grain sample of 10 grams was used for each experiment. After sieving and cleaning, the wheat kernels were cut in half along the longitudinal axis and then mixed with normal kernels at various percentages (by weight) to obtain different partially damaged samples for calibration purposes.

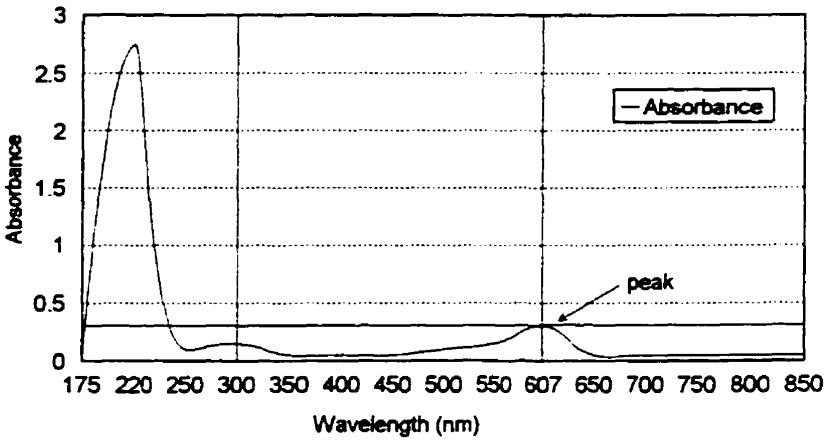

Figure A.1. Peak wavelength of Fast Green FCF dye in aqueous solution of sodium hydroxide.

The partially damaged sample was then soaked in 0.1 % (by weight) Fast Green FCF dye solution for 15 seconds, then rinsed with distilled water, followed by bleaching with 0.05 N sodium hydroxide solution for 60 seconds. The absorbance of the resulting solution was then measured using a *Spectronic 601* spectrophotometer. The spectrophotometer was also calibrated for zero absorbancy with 0.05 N sodium hydroxide solution at 607 nm.

A.2.2.2 Spouting and sampling

In the spouting experiments, wheat kernels were loaded into the bed up to a certain preselected height and the spouting started at time zero. The samples were then sampled at 15 minute intervals. The total spouting time was 165 minutes for each run. The samples were then analyzed using the above colorimetric method. To study the effect of the sampling location, at the end of each experiment 4 samples from different locations in the bed were taken and analyzed.

A.2.2.3 Rewetting

In order to simulate the real drying process of wheat which normally starts at an initial moisture content of about 30 %, a rewetting process is needed since only dried wheat was available. In two experiments, the grains were rewetted in order to investigate the effect of wetness on percent damage. Rewetting was performed by adding precalculated amounts of water to achieve the required initial moisture content and mixing the content thoroughly. The grains were then kept in cold storage with periodic mixing for 72 hours to ensure moisture equilibration.

A.3. Results and Discussion

A.3.1 Calibration curve

The calibration curve of percent absorbance versus percent damaged sample (based on half-cut basis) is presented in Figure A.2. An almost linear relationship is observed. This is expected since the amount of dye in sodium hydroxide solution should be directly proportional to the surface area of exposed internal grains which, in turn, is directly proportional to the percent artificially damaged grains.

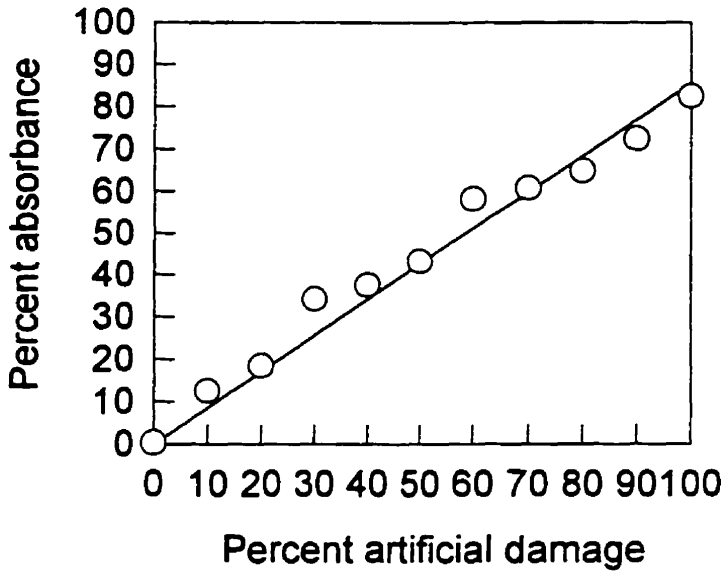

Figure A.2. Calibration curve 1; percent artificial damage versus percent absorbance. $\lambda = 607$ nm.

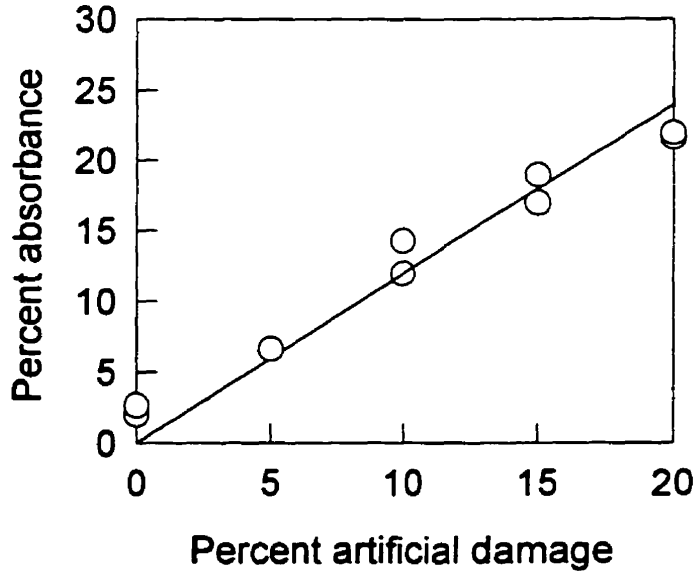

Figure A.3. Calibration curve 2; percent artificial damage versus percent absorbance. $\lambda = 607$ nm.

Analysis of the damage from the first few sets of experiments suggested that percent damage will never exceed 20 % under the operating conditions employed. Therefore, two extra points were added to the calibration curve from 0 to 20 percent. Over this narrower range, the data show a clearer linear relationship between percent absorbance and percent damage (see Figure A.3). Since damage resulting from the spouting experiments appeared to be only in this narrower range, Figure A.3 was used as the calibration curve in this study.

A.3.2 Effect of spouting duration

The increase in grain damage with time seems to follow three main stages; an initial increase in damage in the initial 45 minutes followed by a stage in which damage was almost constant or only increased slightly between 45 to 120 minutes. The final stage was a sharp increase in damage from 120 to 165 minutes. This phenomenon is seen in Figure A.4.

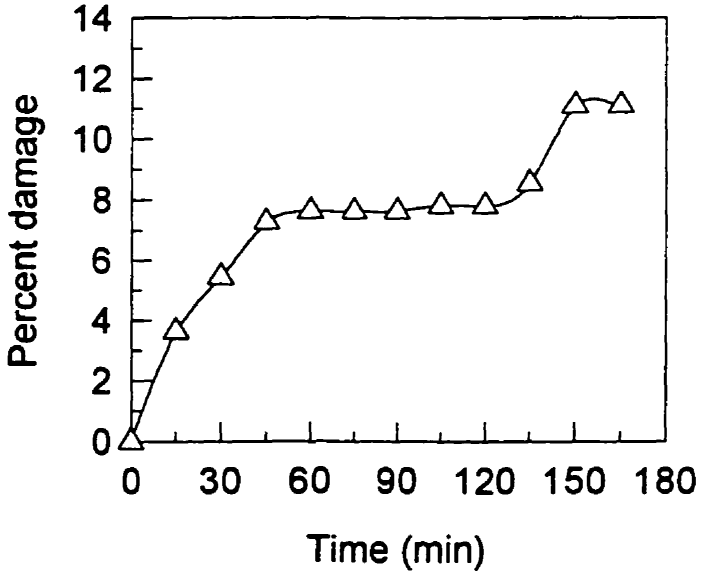

Figure A.4. Effect of spouting duration on percent damage. T_{ig} = 57 °C, U = 0.44 m/s, N = 6 rpm, initial moisture content = 16.4 % d.b.

The expectation that time is a very important variable affecting grain damage during the spouting experiments is confirmed by the results. Longer the time grain kernels spend in the bed, greater is the chance the kernels impacting with the vessel wall as well as other grains. Furthermore, the effect of thermal damage are amplified by longer exposure of grains to heated drying air.

A.3.3 Effect of inlet air temperature

Heat is believed to affect the mechanical properties of wheat kernels and add to the mechanical damage suffered during drying in the spouted bed. The two temperature levels of inlet air chosen for this study were 57 and 80 °C. Temperatures higher than those of interest in practice were chosen as to amplify the effects of inlet air temperature and examine the worse case scenarios.

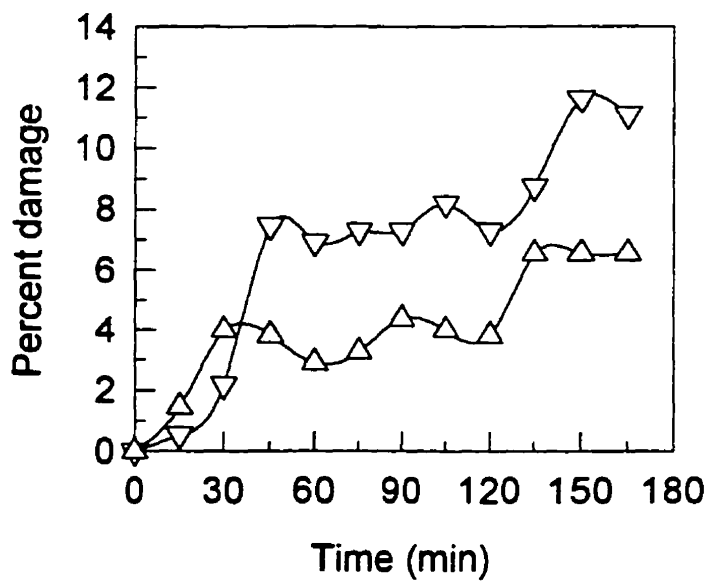

Figure A.5. Effect of inlet air temperature on percent damage (rewetted sample). N = 4 rpm, U = 0.44 m/s, initial moisture content = 29.3 % d.b. Δ, 57 °C; ∇, 80 °C.

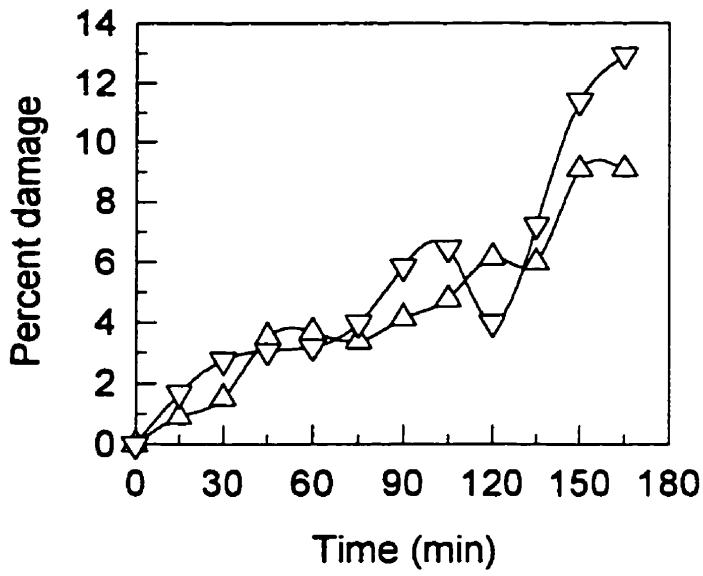

Figure A.6. Effect of inlet air temperature on percent damage (unwetted sample). N = 4 rpm, U = 0.44 m/s, initial moisture content = 16.4 % d.b. Δ , 57 °C; ∇ , 80 ^{0}C.

As can be seen from Figures A.5 and A.6, the effect of inlet air temperature is more pronounced in the case of the rewetted than unwetted grains. It appears that the mechanism of grains damage is closely related to the moisture content and the heat/mass transfer mechanisms inside the kernel. Also observable from these figures is that as the temperature of the drying air was increased grain damage, as expected, also increased.

A.3.4 Effect of air nozzle rotational speed

Two rotational speeds were used to study the effect of the distributor rotational speed, 4 rpm and a higher speed of 6 rpm. As can be seen from Figure A.7, the results show that at the same temperature, the grains spouted at higher rotational speed suffered more damage.

The increase in percent damage with higher rotational speed is expected. Recall that the damage is, to some extent, the result of grains colliding with the vessel wall, bed cover

plate as well as other grains. At higher rotational speed, grains were subjected to more spouting per unit time and resulting in more collisions.

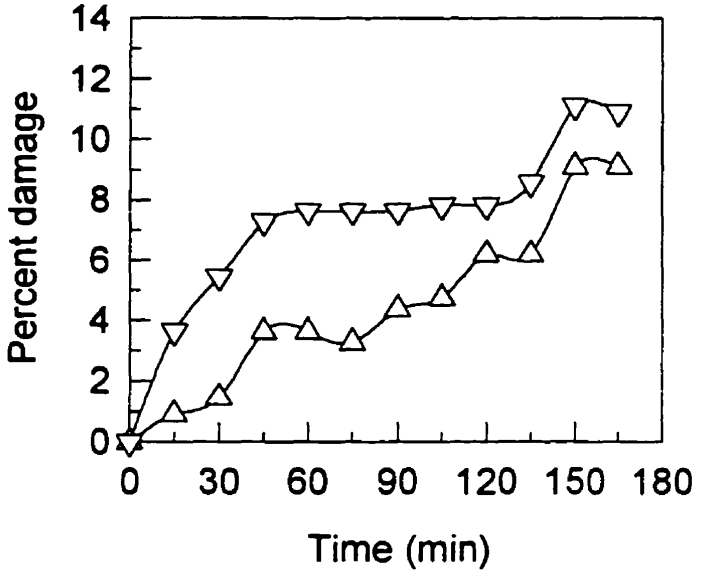

Figure A.7. Effect of air distributor rotational speed. U = 0.44 m/s, T_{ig} = 57 °C, initial moisture content = 16.4 % d.b. Δ ,4 rpm; ∇, 6 rpm.

A.3.5 Effect of inlet air superficial velocity

In order to determine the effect of air flowrate, two different values of air superficial velocity were tested; 0.22 m/s and 0.44 m/s. It can be seen from Figure A.8 that the inlet air velocity has a large effect on grains damage. This trend is expected since at higher air velocity, grains were move and collide at higher speeds.

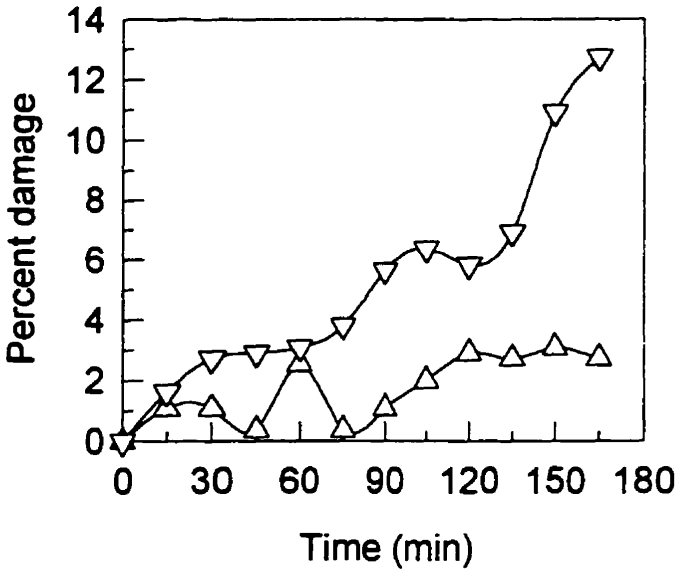

Figure A.8. Effect of inlet air superficial velocity. N = 4 rpm, T_{ig} = 80 °C, initial moisture content = 16.4 % d.b. Δ ,0.22 m/s; ∇, 0.44 m/s.

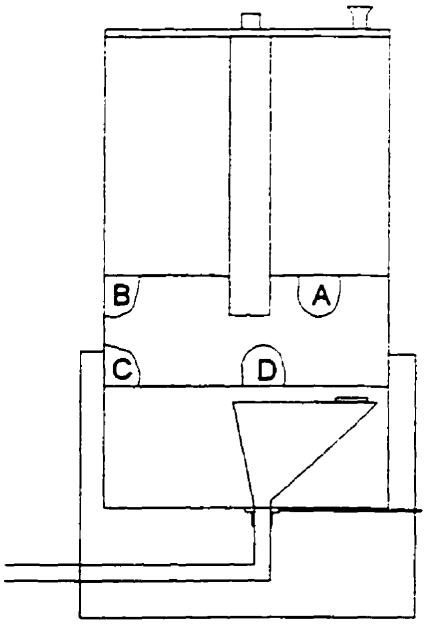

Figure A.9. Sampling locations in the spouted bed.

A.3.6 Effect of sampling location

Four different locations in the bed, as shown in Figure A.9, were chosen to investigate if the damage differed spatially inside the bed. The results showed very little variation, thus confirming that the spouted bed is well-mixed [6].

A.4 Conclusions

Based on a colorimetric technique which relates percent absorbance of a suitable dye to percent mechanical damage of grain kernels. Damage of wheat during drying in a novel rotating-impinging jet spouted bed was examined under various operating conditions. This method has proved reliable to quantify mechanical damage determination within an experimental uncertainty of only 1.1 percent for an artificially damaged sample (calibration process) and 1.5 percent for a sample damaged during spouting.

Nomenclature

B	Breath of wheat kernel, mm
D_p	Effective particle diameter, mm
D_{pe}	Equivalent spherical diameter, mm
D_{pgm}	Geometric particle diameter, mm
L	Length of wheat kernel, mm
N	Air distributor rotational speed, rpm
T_{ig}	Inlet air temperature, °C
U	Inlet air superficial velocity based on column diameter, m s^{-1}
Z	Thickness of wheat kernel, mm

Greek Letters

ε	Voidage, no unit

ϕ Sphericity, no unit

λ wavelength, nm

ρ_b Bulk density, kg m^{-3}

ρ_s True density, kg m^{-3}

References

1. Wall, G.L., Norris, E.R., 1981,"A Technical Note on the use of a Colorimetric Technique for Evaluating Mechanical Corn Kernel Damage", *Can. Agric. Eng.*, 23, pp. 67-68.
2. Schmidt, J.L., Saul, R.A., Steele, J.L., 1976, "Precision of Estimating Mechanical Damage in Shelled Corn", ARS 42-142, *U.S. Department of Agriculture*.
3. Chowdhury, M.H., Buchele, W.F., 1976, "Colorimetric Determination of Grain Damage", *Trans. ASAE*, 19, pp. 807-811.
4. Devahastin, S., Bassila, S., Mujumdar, A.S., Raghavan, G.S.V., "A Colorimetric Technique to Quantify Wheat Grain Damage During Drying", submitted to *Journal of Agricultural Engineering Research*, 1996.
5. Geldart, D., 1973, "Types of Gas Fluidization", *Powder Tech.*, 7, pp. 285-292.
6. Jumah, R.Y., 1995, "Flow and Drying Characteristics of a Rotating Jet Spouted Bed", Ph.D. Thesis, McGill University, Canada.

IMAGE EVALUATION
TEST TARGET (QA-3)

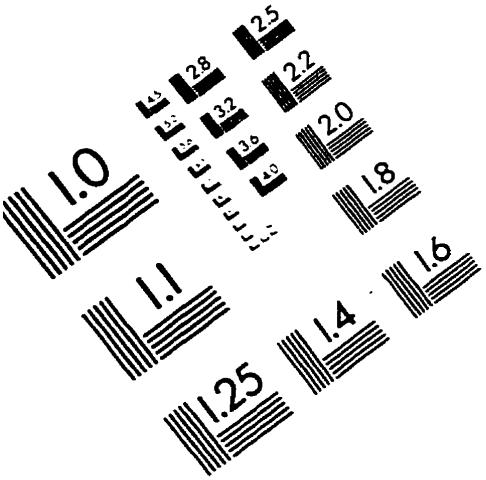

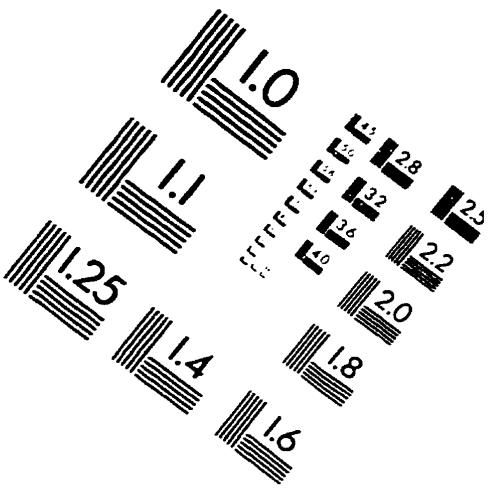

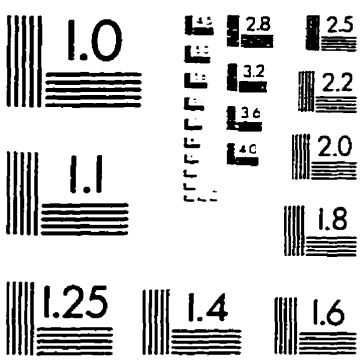

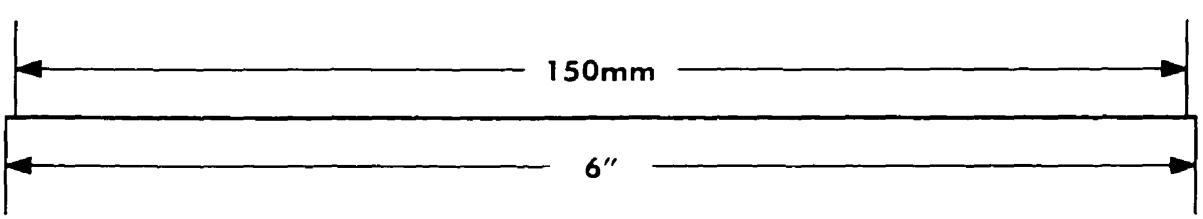

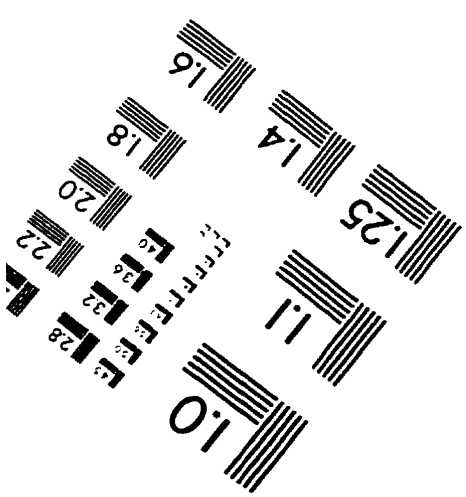

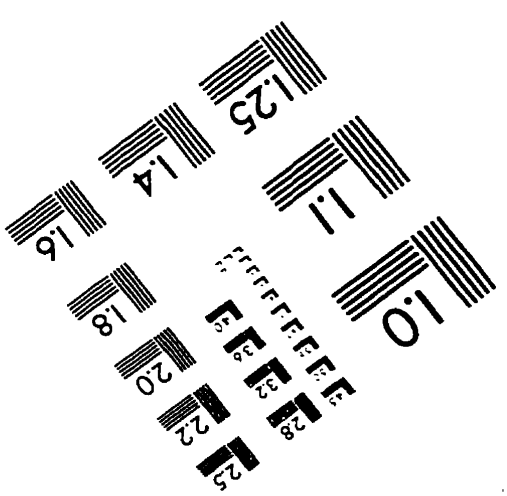

APPLIED IMAGE, Inc
1653 East Main Street
Rochester, NY 14609 USA
Phone: 716/482-0300
Fax: 716/288-5989